Manuscript submitted to
AIMS' Journals
Volume **00**, Number **0**, Xxxx **XXXX**

Website: http://AIMsciences.org

pp. **000–000**

AN ASYMPTOTIC ANALYSIS OF THE PERSISTENCE THRESHOLD FOR THE DIFFUSIVE LOGISTIC MODEL IN SPATIAL ENVIRONMENTS WITH LOCALIZED PATCHES

A.E. Lindsay and M.J. Ward

Mathematics Department
University of British Columbia
Vancouver, B.C.
Canada, V6T 1Z4

(Communicated by Yuan Lou)

Abstract. An indefinite weight eigenvalue problem characterizing the threshold condition for extinction of a population based on the single-species diffusive logistic model in a spatially heterogeneous environment is analyzed in a bounded two-dimensional domain with no-flux boundary conditions. In this eigenvalue problem, the spatial heterogeneity of the environment is reflected in the growth rate function, which is assumed to be concentrated in n small circular disks, or portions of small circular disks, that are contained inside the domain. The constant bulk or background growth rate is assumed to be spatially uniform. The disks, or patches, represent either strongly favorable or strongly unfavorable local habitats. For this class of piecewise constant bang-bang growth rate function, an asymptotic expansion for the persistence threshold λ_1, representing the positive principal eigenvalue for this indefinite weight eigenvalue problem, is calculated in the limit of small patch radii by using the method of matched asymptotic expansions. By analytically optimizing the coefficient of the leading-order term in the asymptotic expansion of λ_1, general qualitative principles regarding the effect of habitat fragmentation are derived. In certain degenerate situations, it is shown that the optimum spatial arrangement of the favorable habit is determined by a higher-order coefficient in the asymptotic expansion of the persistence threshold.

1. **Introduction.** The diffusive logistic model, which describes the evolution of a population with density $u(x,t)$ diffusing with constant diffusivity $D = 1/\lambda > 0$ throughout some habitat represented by a bounded domain $\Omega \subset \mathbb{R}^2$, is formulated as

$$u_t = \Delta u + \lambda u\left[m(x) - u\right], \quad x \in \Omega\,; \qquad \partial_n u = 0\,, \quad x \in \partial\Omega\,; \tag{1.1a}$$

$$u(x,0) = u_0(x) \geq 0\,, \qquad x \in \Omega\,. \tag{1.1b}$$

The no-flux boundary condition in (1.1a) specifies that no individuals cross the boundary of the habitat Ω. The initial population density $u_0(x)$ is non-negative and not identically zero. The function $m(x)$ represents the growth rate for the species,

2000 *Mathematics Subject Classification.* Primary: 35B25 , 35P99; Secondary: 92B99.

Key words and phrases. Persistence, Singular Asymptotic Expansions, Neumann Green's Function.

with $m(x) > 0$ in favorable parts of the habitat, and $m(x) < 0$ in unfavorable parts of the habitat. The integral $\int_\Omega m\,dx$ measures the total resources available in the spatially heterogeneous environment. With respect to applications in ecology, this model was first formulated in [26].

To determine the stability of the extinction equilibrium solution $u = 0$, we set $u = \phi(x)e^{-\sigma t}$ in (1.1), where $\phi(x) \ll 1$, to obtain that ϕ satisfies

$$\Delta\phi + \lambda m(x)\phi = -\sigma\phi\,, \quad x \in \Omega; \qquad \partial_n\phi = 0\,, \quad x \in \partial\Omega\,. \tag{1.2}$$

The threshold for species persistence is determined by the stability border of the extinct solution $u = 0$. At this bifurcation point, the eigenvalue of the linearized problem about the zero solution must pass through zero. Therefore, by setting $\sigma = 0$ in (1.2) the problem reduces to the determination of a scalar λ and a function ϕ that satisfies the indefinite weight eigenvalue problem

$$\Delta\phi + \lambda m(x)\phi = 0\,, \quad x \in \Omega\,; \qquad \partial_n\phi = 0\,, \quad x \in \partial\Omega\,; \qquad \int_\Omega \phi^2\,dx = 1\,. \tag{1.3}$$

We say that $\lambda_1 > 0$ is a positive principal eigenvalue of (1.3) if the corresponding eigenfunction ϕ_1 of (1.3) is positive in Ω. It is well-known (cf. [2], [13], [25]) that (1.3) has a unique positive principal eigenvalue λ_1 if and only if $\int_\Omega m\,dx < 0$ and the set $\Omega^+ = \{x \in \Omega\ ;\ m(x) > 0\}$ has positive measure. Such an eigenvalue is the smallest positive eigenvalue of (1.3).

The positive principal eigenvalue λ_1 is interpreted as the persistence threshold for the species. It is well-known that if $\lambda < \lambda_1$, then $u(x,t) \to 0$ uniformly in $\bar\Omega$ for all non-negative and non-trivial initial data, so that the population tends to extinction. Alternatively, if $\lambda > \lambda_1$, then $u(x,t) \to u^*(x)$ uniformly in $\bar\Omega$ as $t \to \infty$, where u^* is the unique positive steady-state solution of (1.1). For this range of λ the species will persist. Many mathematical results for (1.1) under different boundary conditions are given in the pioneering works of [4], [5], and [6]. Related results for multi-species interactions and other mathematical problems in ecology are given in [7] (see also the survey article of [18]).

An interesting problem in mathematical ecology is to determine, among all functions $m(x)$ for which a persistence threshold exists, which $m(x)$ yields the smallest λ_1 for a fixed amount of total resources $\int_\Omega m\,dx$. In other words, we seek to determine the optimum arrangement of favorable habitats in Ω in order to allow the species to persist for the largest possible diffusivity D. This optimization problem was originally posed and studied in [4] and [6]. For (1.1) under Neumann boundary conditions in a two-dimensional domain Ω, it was proved in Theorem 1.1 of [17] that the optimum $m(x)$ is piecewise continuous and of bang-bang type. An earlier result showing the existence of a similar bang-bang optimal control for $m(x)$ for the

Dirichlet problem was given in [4]. For (1.1) posed in a one-dimensional interval $0 < x < 1$, it was proved in Theorem 1.2 of [17] that the optimal $m(x)$ consists of a single favorable habitat attached to one of the two endpoints of the interval. Related results were given in [6] under Dirichlet, Neumann, or Robin type boundary conditions.

The minimization of λ_1 in cylindrical domains was studied in [14]. For a rectangular domain, it was shown in [14] that if $|\int_\Omega m(x)\,dx|$ is below some threshold value, then the optimum λ_1 occurs when the favorable habitat is concentrated near one of the four corners of the domain. Otherwise, the optimum λ_1 occurs when the favorable habitat is attached to either of the two ends of the domain with the shortest edge. For spatially periodic environments, the effect of fragmentation of the favorable resources was studied in [1] using Steiner symmetrization, and some results were obtained for Dirichlet boundary conditions. Related applications of this symmetrization approach was given in [16]. A treatise on the modeling of biological invasions in periodic spatial environments is given [24]. In [22] stochastic methods were used to determine the persistence threshold for the diffusive logistic model for an infinitely periodic heterogeneous media. This study, which eliminated the effect of boundary conditions, showed that habitat fragmentation decreases the persistence of the species. For (1.1) in a bounded two-dimensional domain with Neumann boundary conditions, the existence of an optimal configuration for $m(x)$ was proved in [21]. In [21], the growth rate function $m(x)$ was chosen to be of bang-bang type, in accordance with Theorem 1.1 of [17] described above. By distributing the favorable and unfavorable habitats on a grid, and then letting the grid-spacing decrease, it was shown both numerically and analytically in [21] that the globally optimal favorable spatial habitat configuration is either ball-shaped or stripe-shaped, depending on the amount of available resources.

Although these previous studies give considerable insight into the effect of spatial fragmentation of habitat resources on the persistence threshold in specific situations, such as cylindrical domains or periodic environments, the problem of the optimum choice for $m(x)$ in arbitrary two-dimensional domains with no periodicity assumption is largely an open problem.

The goal of this paper is to asymptotically calculate, and then optimize, the persistence threshold λ_1 for a particular class of piecewise constant growth rate function $m = m_\varepsilon(x)$ in an arbitrary two-dimensional domain. We assume that $m_\varepsilon(x)$ is localized to n small circular patches of radii $\mathcal{O}(\varepsilon)$, each of which is centered either inside Ω or on $\partial\Omega$. We assume that the boundary $\partial\Omega$ is piecewise differentiable, but allow for the domain boundary to have a finite numbers of corners, each with

a non-zero contact angle, which arises from a jump discontinuity of the slope of the tangent line to the boundary. We denote $\Omega^I \equiv \{x_1,\dots,x_n\}\cap\Omega$ to be the set of the centers of the interior patches, while $\Omega^B \equiv \{x_1,\dots,x_n\}\cap\partial\Omega$ is the set of the centers of the boundary patches. We assume that the patches are well-separated in the sense that $|x_i - x_j| \gg \mathcal{O}(\varepsilon)$ for $i \neq j$ and that the interior patches are not too close to the boundary, i.e. $\text{dist}(x_j,\partial\Omega) \gg \mathcal{O}(\varepsilon)$ whenever $x_j \in \Omega^I$. To accommodate a boundary patch, we will associate with each x_j for $j = 1,\dots,n$, an angle $\pi\alpha_j$ representing the angular fraction of a circular patch that is contained within Ω. More specifically, $\alpha_j = 2$ whenever $x_j = \Omega^I$, $\alpha_j = 1$ when $x_j \in \Omega^B$ and x_j is a point where $\partial\Omega$ is smooth, and $\alpha_j = 1/2$ when $x_j \in \partial\Omega$ is at a corner point of $\partial\Omega$ for which the two (one-sided) tangent lines to the boundary intersect at a $\pi/2$ contact angle (see Fig. 1). The growth rate function $m = m_\varepsilon(x)$ in (1.3) is taken to have the specific form

$$m = m_\varepsilon(x) \equiv \begin{cases} m_j/\varepsilon^2\,, & x \in \Omega_{\varepsilon_j}\,, \quad j = 1,\dots,n\,, \\ -m_b\,, & x \in \Omega\backslash\bigcup_{j=1}^n \Omega_{\varepsilon_j}\,. \end{cases} \tag{1.4}$$

Here $\Omega_{\varepsilon_j} \equiv \{x\,|\,|x - x_j| \le \varepsilon\rho_j \cap \Omega\}$, so that each patch Ω_{ε_j} is the portion of a circular disk of radius $\varepsilon\rho_j$ that is strictly inside Ω. The constant m_j is the local growth rate of the j^{th} patch, with $m_j > 0$ for a favorable habitat and $m_j < 0$ for an unfavorable habitat. The constant $m_b > 0$ is the background bulk decay rate for the unfavorable habitat. In terms of this growth rate function, the condition of [2], [13], and [25] for the existence of a persistence threshold is that one of the m_j for $j = 1,\dots,n$ must be positive, and that the following asymptotically valid inequality on the total resources hold as $\varepsilon \to 0$:

$$\int_\Omega m_\varepsilon\,dx = -m_b|\Omega| + \frac{\pi}{2}\sum_{j=1}^n \alpha_j m_j \rho_j^2 + \mathcal{O}(\varepsilon^2) < 0\,. \tag{1.5}$$

Here $|\Omega|$ denotes the area of Ω. We assume that the parameters are chosen so that (1.5) is satisfied. A schematic plot of a domain with interior circular patches, and with portions of circular patches on its boundary, is shown in Fig. 1.

This specific form for $m_\varepsilon(x)$ is motivated by Theorem 1.1 of [17] that states that the optimal growth rate function must be of bang-bang type, and the result of [21] that shows that a sufficiently small optimum favorable habitat must be a circular disk.

In §2 the method of matched asymptotic expansions is used to derive a two-term asymptotic expansion for the persistence threshold λ_1 for the case of either a single favorable interior or boundary habitat. The asymptotic analysis is extended in §3 to asymptotically calculate λ_1 for (1.3) with growth rate function (1.4), which allows

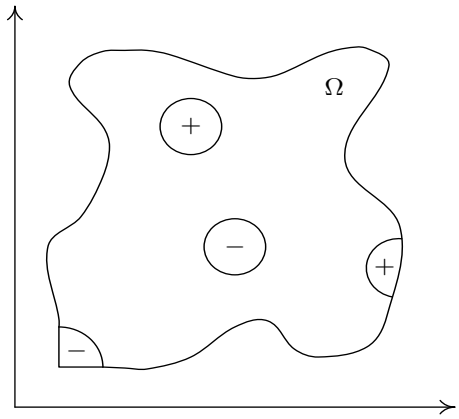

FIGURE 1. Schematic plot of a two-dimensional domain Ω with localized strongly favorable (+) or unfavorable (−) habitats, or patches, as described by (1.4). The patches inside the domain are small circular disks. On the domain boundary, the patches are the portions of circular disks that lie within the domain. The unfavorable boundary habitat in the lower left part of this figure is at a $\pi/2$ corner of $\partial\Omega$.

for multiple interior or boundary habitats. Our analysis, which is summarized in Principal Result 3.1 of §3, shows that λ_1 has the two-term asymptotic expansion

$$\lambda_1 = \mu_0\nu + \nu^2\mu_1(x_1,\dots,x_n) + \mathcal{O}(\nu^3)\,, \qquad \nu(\varepsilon) = -1/\log\varepsilon\,. \tag{1.6}$$

Here the leading-order coefficient μ_0 is the unique positive root of $\mathcal{B}(\mu_0) = 0$ on $0 < \mu_0 < 2/(m_J\rho_J^2)$, where

$$\mathcal{B}(\mu_0) \equiv -m_b|\Omega| + \pi\sum_{j=1}^{n}\frac{\alpha_j m_j\rho_j^2}{2 - m_j\rho_j^2\mu_0}\,, \qquad m_J\rho_J^2 \equiv \max_{m_j>0}\{m_j\rho_j^2\,|\,j=1,\dots,n\}\,. \tag{1.7}$$

The coefficient μ_1, which depends explicitly on the spatial configuration $\{x_1,\dots,x_n\}$ of patches, is determined in terms of a matrix involving the Neumann Green's function and the surface Neumann Green's function for Ω.

In §4 we study the effect of fragmentation of resources on the coefficients μ_0 and μ_1 in the asymptotic expansion of the persistence threshold. For a prescribed amount of resources, for which $\int_\Omega m_\varepsilon\,dx$ in (1.5) is fixed, we seek to determine the patch configuration that minimizes μ_0, or in certain degenerate situations, minimizes the coefficient μ_1 in (1.6).

From an analysis based on the leading-order coefficient μ_0 in (1.6), in §4.2 we derive some sufficient conditions characterizing the effect of habitat fragmentation on the persistence threshold. There are several key qualitative principles that are established. Firstly, the fragmentation of a favorable interior habitat into two smaller

favorable interior habitats is shown to be deleterious to species persistence, whereas the migration of an interior favorable habitat to the boundary of the domain is always advantageous. The optimal boundary location to concentrate a favorable resource is at a corner of the domain boundary with the smallest contact angle, provided that this angle is less than π. Secondly, the fragmentation of a favorable interior habitat into a smaller favorable interior habitat together with a favorable boundary habitat is advantageous to species persistence only when the boundary habitat is sufficiently strong. Further general principles, based on the optimization of μ_0, are summarized in Qualitative Results I–III of §4.2. An illustration of these principles for certain patch distributions in the unit disk is given in §4.

In §4 we also show that in certain degenerate situations, the problem of determining the optimal location for a favorable resource requires the examination of the coefficient μ_1 of the second term in the asymptotic expansion of λ_1. In particular, such a problem occurs in optimizing λ_1 with respect to the boundary location of a single favorable boundary patch in a domain with a smooth boundary. In this case, we show in Principal Result 4.1 that λ_1 is minimized when the boundary patch is centered at a point $x_0 \in \partial\Omega$ at which the regular part of the surface Neumann Green's function attains its global maximum value on the boundary. The relationship between the global maximum of the boundary curvature and the regular part of the surface Neumann Green's function for smooth perturbations of the unit disk is investigated in Principal Results 4.2 and 4.3 of §4.

In §4.3 we consider the optimization of λ_1 for the case where an additional favorable resource is to be located inside a domain that has a pre-existing and fixed patch distribution. In this case, we show in §4.3 that the optimization of λ_1 typically requires the examination of the coefficient μ_1 of the second-order term in the asymptotic expansion of λ_1. The theory in §4.3 is illustrated for two specific examples involving the unit disk and the unit square, for which the required Green's functions are known analytically. Finally, a brief discussion is given in §5.

Related problems involving the asymptotic calculation and optimization of the fundamental eigenvalue of the Laplacian have been studied in perforated two-dimensional domains (cf. [9], [15], [19], [27], and [28]), in two-dimensional domains with perforated boundaries (cf. [3], [10], [11], [20]), and under the effect of strongly localized potentials (cf. [12], [28]).

2. **Determination of the Persistence Threshold for One Patch.**

In this section we use the method of matched asymptotic expansions to derive a two-term asymptotic expansion for the positive principal eigenvalue λ of (1.3) for the case of

one localized favorable habitat centered at either a point interior to Ω or a point on $\partial\Omega$.

2.1. **A Single Interior Patch.** We first consider the case of one interior circular patch centered at $x_0 \in \Omega$, with $\mathrm{dist}(x_0, \partial\Omega) \gg \mathcal{O}(\varepsilon)$. We asymptotically calculate the positive principal eigenvalue $\lambda > 0$ and corresponding eigenfunction $\phi > 0$ of

$$\Delta\phi + \lambda\, m_\varepsilon(x)\phi = 0\,, \quad x \in \Omega; \qquad \partial_n\phi = 0\,, \quad x \in \partial\Omega\,; \qquad \int_\Omega \phi^2\, dx = 1\,, \tag{2.1a}$$

in the small patch radius limit $\varepsilon \to 0$, where the growth rate function $m_\varepsilon(x)$ is defined as

$$m_\varepsilon(x) = \begin{cases} m_+/\varepsilon^2\,, & x \in \Omega_{\varepsilon_0}\,, \\ -m_b, & x \in \Omega\backslash\Omega_{\varepsilon_0}\,. \end{cases} \tag{2.1b}$$

Here the patch Ω_{ε_0} is the circular disk $\Omega_{\varepsilon_0} \equiv \{x \,|\, |x - x_0| \le \varepsilon\,\}$. In (2.1b), $m_+ > 0$ is the local growth rate of the favorable habitat, while $m_b > 0$ gives the background bulk decay rate for the unfavorable habitat.

The condition $\int_\Omega m\, dx < 0$ for the existence of a positive principal eigenvalue is asymptotically equivalent to

$$\int_\Omega m\, dx = -m_b|\Omega| + \pi m_+ + \mathcal{O}(\varepsilon^2) < 0\,, \tag{2.2}$$

in the limit $\varepsilon \to 0$. We assume that m_b and m_+ are chosen so that this condition holds.

We expand the positive principal eigenvalue λ of (2.1) as

$$\lambda \sim \mu_0\nu + \mu_1\nu^2 + \cdots\,, \qquad \nu = -1/\log\varepsilon\,, \tag{2.3}$$

for some coefficients μ_0 and μ_1 to be found. In the outer region, defined away from an $\mathcal{O}(\varepsilon)$ neighborhood of x_0, we expand the corresponding eigenfunction as

$$\phi \sim \phi_0 + \nu\phi_1 + \nu^2\phi_2 + \cdots\,. \tag{2.4}$$

Upon substituting (2.3) and (2.4) into (2.1), we obtain that ϕ_0 is a constant. The normalization condition $\int_\Omega \phi_0^2\, dx = 1$ yields $\phi_0 = |\Omega|^{-1/2}$, where $|\Omega|$ is the area of Ω. In addition, we obtain that ϕ_1 and ϕ_2 satisfy

$$\Delta\phi_1 = \mu_0 m_b\phi_0\,, \quad x \in \Omega\backslash\{x_0\}\,; \qquad \partial_n\phi_1 = 0\,, \quad x \in \partial\Omega\,; \qquad \int_\Omega \phi_1\, dx = 0\,, \tag{2.5a}$$

$$\Delta\phi_2 = \mu_1 m_b\phi_0 + \mu_0 m_b\phi_1\,, \quad x \in \Omega\backslash\{x_0\}\,; \qquad \partial_n\phi_2 = 0\,, \quad x \in \partial\Omega\,; \qquad \int_\Omega \left(\phi_1^2 + 2\phi_0\phi_2\right)\, dx = 0\,. \tag{2.5b}$$

The matching of ϕ_1 and ϕ_2 to an inner solution defined in an $\mathcal{O}(\varepsilon)$ neighborhood of the patch at x_0, as done below, will yield singularity conditions for ϕ_1 and ϕ_2 as $x \to x_0$.

In the inner region near the patch centered at x_0 we introduce the local variables y and ψ by

$$y = \varepsilon^{-1}(x - x_0)\,, \qquad \psi(y) = \phi(x_0 + \varepsilon y)\,. \tag{2.6}$$

Then, (2.1) becomes

$$\Delta\psi = \begin{cases} -\lambda m_+ \psi\,, & |y| < 1\,, \\ \mathcal{O}(\varepsilon^2)\,, & |y| > 1\,. \end{cases} \tag{2.7}$$

We then represent the inner approximation to the eigenfunction as

$$\psi \sim \psi_0 + \nu\psi_1 + \nu^2\psi_2 + \cdots\,, \qquad \nu = -1/\log\varepsilon\,. \tag{2.8}$$

We substitute (2.8) and (2.3) into (2.7), and collect powers of ν, to obtain that ψ_0 is an unknown constant, and that ψ_1 and ψ_2 satisfy

$$\Delta\psi_k = \begin{cases} \mathcal{F}_k\,, & |y| \le 1\,, \\ 0\,, & |y| \ge 1\,. \end{cases} \tag{2.9a}$$

Here $\mathcal{F}_k$ for $k = 1, 2$ is defined by

$$\mathcal{F}_1 = -\mu_0 m_+ \psi_0\,, \qquad \mathcal{F}_2 = -\mu_0 m_+ \psi_1 - \mu_1 m_+ \psi_0\,. \tag{2.9b}$$

We then calculate the solution ψ_1 to (2.9) as

$$\psi_1 = \begin{cases} A_1\rho^2/2 + \bar{\psi}_1\,, & \rho \le 1\,, \\ A_1\log\rho + \frac{A_1}{2} + \bar{\psi}_1\,, & \rho \ge 1\,, \end{cases} \tag{2.10a}$$

where $\rho = |y|$. Here $\bar{\psi}_1$ is an unknown constant, and A_1 is given by

$$A_1 = \frac{\mathcal{F}_1}{2} = -\frac{1}{2}\mu_0 m_+ \psi_0\,. \tag{2.10b}$$

In addition, for the solution ψ_2 to (2.9) we calculate its far-field behavior as

$$\psi_2 \sim A_2\log\rho + \mathcal{O}(1)\,, \quad \text{as} \quad \rho \to \infty\,, \qquad A_2 \equiv \int_0^1 \mathcal{F}_2\,\rho\,d\rho\,. \tag{2.11a}$$

We then calculate A_2 by using (2.10) and (2.9b) for $\mathcal{F}_2$ to get

$$A_2 = -\mu_0 m_+ \int_0^1 \left(A_1\frac{\rho^2}{2} + \bar{\psi}_1\right)\rho\,d\rho - \frac{1}{2}\mu_1 m_+\psi_0 = \frac{A_1}{\psi_0}\left(\frac{A_1}{4} + \bar{\psi}_1 + \frac{\mu_1}{\mu_0}\psi_0\right)\,. \tag{2.11b}$$

The matching condition is that the near-field behavior as $x \to x_0$ of the outer representation of the eigenfunction must agree asymptotically with the far-field behavior of the inner eigenfunction as $|y| = \varepsilon^{-1}|x - x_0| \to \infty$, so that

$$\phi_0 + \nu\phi_1 + \nu^2\phi_2 + \cdots \sim \psi_0 + \nu\psi_1 + \nu^2\psi_2 + \cdots\,. \tag{2.12}$$

Upon using the far-field behavior of ψ_1 and ψ_2, as given in (2.10) and (2.11) respectively, we obtain that (2.12) becomes

$$\phi_0+\nu\phi_1+\nu^2\phi_2+\cdots\sim\psi_0+A_1+\nu\left(A_1\log|x-x_0|+\frac{A_1}{2}+\bar{\psi}_1+A_2\right)+\nu^2\left(A_2\log|x-x_0|+\mathcal{O}(1)\right)\,. \tag{2.13}$$

Since ϕ_0 and ψ_0 are constants, we obtain the first matching condition that

$$\phi_0=\psi_0+A_1\,. \tag{2.14}$$

Then, from the $\mathcal{O}(\nu)$ terms in the matching condition (2.13), we obtain that ϕ_1 satisfies (2.5a) subject to the singularity behavior

$$\phi_1\sim A_1\log|x-x_0|+\frac{A_1}{2}+\bar{\psi}_1+A_2\,,\quad\text{as}\quad x\to x_0\,. \tag{2.15}$$

We remark that the singularity behavior in (2.15) specifies both the regular and singular part of a Coulomb singularity. Consequently, this singularity structure provides one constraint relating A_1, A_2, and $\bar{\psi}_1$.

The problem for ϕ_1 can be written in terms of the Dirac distribution as

$$\Delta\phi_1=\mu_0 m_b\phi_0+2\pi A_1\delta(x-x_0)\,,\quad x\in\Omega\,;\qquad \partial_n\phi_1=0\,,\quad x\in\partial\Omega\,. \tag{2.16}$$

The divergence theorem then yields

$$A_1=-\frac{1}{2\pi}\left(\mu_0 m_b|\Omega|\phi_0\right)\,. \tag{2.17}$$

Next, we write the solution to (2.16) in terms of the Neumann Green's function $G(x;x_0)$ as

$$\phi_1=-2\pi A_1 G(x;x_0)=\mu_0 m_b|\Omega|\phi_0 G(x;x_0)\,. \tag{2.18}$$

Here $G(x;x_0)$ is the unique solution to

$$\Delta G=\frac{1}{|\Omega|}-\delta(x-x_0)\,,\quad x\in\Omega\,;\qquad \partial_n G=0\,,\quad x\in\partial\Omega\,;\qquad \int_\Omega G\,dx=0\,, \tag{2.19a}$$

$$G(x;x_0)\sim-\frac{1}{2\pi}\log|x-x_0|+R(x_0;x_0)\,,\quad\text{as}\quad x\to x_0\,, \tag{2.19b}$$

where $R(x_0;x_0)$ is the regular part of $G(x;x_0)$ at $x=x_0$. By expanding ϕ_1 in (2.18) as $x\to x_0$ and equating the non-singular part of the resulting expression with that of (2.15), we obtain

$$-2\pi A_1 R(x_0;x_0)=\frac{A_1}{2}+\bar{\psi}_1+A_2\,. \tag{2.20}$$

Finally, we obtain from the $\mathcal{O}(\nu^2)$ terms in the matching condition (2.13) that $\phi_2\sim A_2\log|x-x_0|$ as $x\to x_0$, where ϕ_2 is the solution to (2.5b). In terms of the Dirac mass, this problem for ϕ_2 can be written as

$$\Delta\phi_2=\mu_1 m_b\phi_0+\mu_0 m_b\phi_1+2\pi A_2\delta(x-x_0)\,,\quad x\in\Omega\,;\qquad \partial_n\phi_2=0\,,\quad x\in\partial\Omega\,, \tag{2.21}$$

with normalization condition $\int_\Omega \left(\phi_1^2 + 2\phi_0\phi_2\right)\,dx = 0$. The divergence theorem, together with $\int_\Omega \phi_1\,dx = 0$, then yields that

$$2\pi A_2 = -\mu_1 m_b |\Omega|\phi_0\,. \tag{2.22}$$

The leading-order eigenvalue correction μ_0 is obtained by combining (2.14) and (2.17), together with using $A_1 = -\mu_0 m_+\psi_0/2$ from (2.10b). This yields that

$$\phi_0 = \frac{\pi m_+}{|\Omega| m_b}\psi_0\,, \qquad \phi_0 = \left(1 - \frac{\mu_0 m_+}{2}\right)\psi_0\,. \tag{2.23}$$

Therefore, since $\phi_0 = |\Omega|^{-1/2}$, we obtain

$$\mu_0 = \frac{2}{m_+}\left[1 - \frac{\pi m_+}{|\Omega| m_b}\right], \qquad \psi_0 = \frac{|\Omega| m_b}{\pi m_+}\phi_0\,, \qquad \phi_0 = |\Omega|^{-1/2}\,. \tag{2.24}$$

Since $\int_\Omega m\,dx < 0$, then $m_+\pi/(|\Omega| m_b) < 1$ from (2.2). Consequently, it follows from (2.24) that $\mu_0 > 0$. Next, we combine (2.17) and (2.22) to evaluate the ratio A_2/A_1 as $A_2/A_1 = \mu_1/\mu_0$. Upon using $A_2/A_1 = \mu_1/\mu_0$ in (2.20) and (2.11b), we readily determine $\bar{\psi}_1$ and the eigenvalue correction μ_1 as

$$\bar{\psi}_1 = -\frac{A_1}{4}\,, \qquad \mu_1 = -\left(\frac{1}{4} + 2\pi R(x_0;x_0)\right)\mu_0\,. \tag{2.25}$$

Finally, a two-term expansion for the eigenfunction in the outer region is obtained from (2.4) by using (2.18) for ϕ_1. The corresponding two-term inner approximation to the eigenfunction is given by (2.8), where ψ_1 is given in (2.10) with $\bar{\psi}_1 = -A_1/4$. We summarize our result as follows:

Principal Result 2.1: *In the limit of small patch radius, $\varepsilon \to 0$, the positive principal eigenvalue λ of (2.1) has the following two-term asymptotic expansion in terms of the logarithmic gauge function $\nu = -1/\log\varepsilon$:*

$$\lambda = \mu_0\nu - \mu_0\nu^2\left[\frac{1}{4} + 2\pi R(x_0;x_0)\right] + \mathcal{O}(\nu^3)\,; \qquad \mu_0 \equiv \frac{2}{m_+}\left[1 - \frac{\pi m_+}{|\Omega| m_b}\right]. \tag{2.26a}$$

A two-term asymptotic expansion for the corresponding eigenfunction in the outer region $|x - x_0| \gg \mathcal{O}(\varepsilon)$ is

$$\phi \sim \phi_0\left(1 + \nu\mu_0 m_b|\Omega| G(x;x_0)\right)\,. \tag{2.26b}$$

Here $G(x;x_0)$ is the Neumann Green's function of (2.19) with regular part $R(x_0;x_0)$. The corresponding inner approximation to the eigenfunction, with $y = \varepsilon^{-1}(x - x_0)$ and $\rho = |y| = \mathcal{O}(1)$, is

$$\psi \sim \frac{m_b|\Omega|}{m_+\pi}\phi_0\left(1 - \frac{\mu_0 m_+}{2}\nu\tilde{\psi}_1(\rho)\right)\,, \tag{2.26c}$$

where $\phi_0 = |\Omega|^{-1/2}$, and $\tilde{\psi}_1(\rho)$ is defined by

$$\tilde{\psi}_1(\rho) \equiv \begin{cases} \rho^2/2 - 1/4\,, & \rho \le 1\,, \\ \log\rho + 1/4\,, & \rho \ge 1\,. \end{cases} \tag{2.26d}$$

The eigenvalue problem (2.1) is explicitly solvable only for the special case where Ω is the unit disk with a circular patch of radius ε centered at the origin. For this special case, the solution to (2.1), which is continuous across the patch boundary $r=\varepsilon$, is

$$\phi = \begin{cases} C\left[I_0\left(\sqrt{\lambda m_b}r\right) - \dfrac{I_0'\left(\sqrt{\lambda m_b}\right)}{K_0'\left(\sqrt{\lambda m_b}\right)}K_0\left(\sqrt{\lambda m_b}r\right)\right], & \varepsilon \le r \le 1\,, \\ C\left[I_0\left(\sqrt{\lambda m_b}\varepsilon\right) - \dfrac{I_0'\left(\sqrt{\lambda m_b}\right)}{K_0'\left(\sqrt{\lambda m_b}\right)}K_0\left(\sqrt{\lambda m_b}\varepsilon\right)\right]\dfrac{J_0\left(\sqrt{\lambda m_+}r/\varepsilon\right)}{J_0\left(\sqrt{\lambda m_+}\right)}, & 0 \le r \le \varepsilon\,. \end{cases} \tag{2.27}$$

Here $I_0(z)$ and $K_0(z)$ are the modified Bessel functions of the first and second kind of order zero. By imposing that ϕ is smooth across $r=\varepsilon$, and recalling that $J_0'(z) = -J_1(z)$, $I_0'(z) = I_1(z)$ and $K_0'(z) = -K_1(z)$, we obtain the following transcendental equation for λ:

$$\varepsilon\sqrt{\frac{m_b}{m_+}}\frac{J_0\left(\sqrt{\lambda m_+}\right)}{J_1\left(\sqrt{\lambda m_+}\right)} = \frac{K_0\left(\sqrt{\lambda m_b}\varepsilon\right)I_1\left(\sqrt{\lambda m_b}\right) + K_1\left(\sqrt{\lambda m_b}\right)I_0\left(\sqrt{\lambda m_b}\varepsilon\right)}{K_1\left(\sqrt{\lambda m_b}\varepsilon\right)I_1\left(\sqrt{\lambda m_b}\right) - K_1\left(\sqrt{\lambda m_b}\right)I_1\left(\sqrt{\lambda m_b}\varepsilon\right)}\,. \tag{2.28}$$

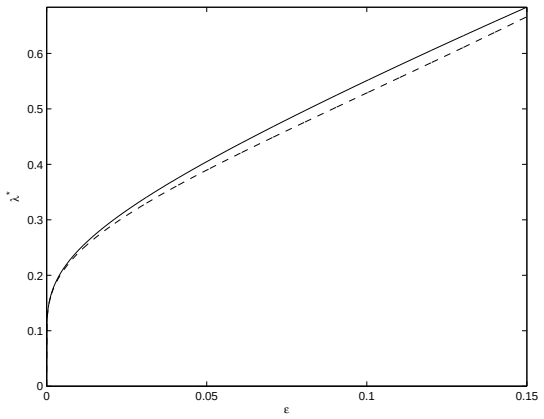

FIGURE 2. Plot of the two-term asymptotic expansion (dashed curve) (2.29) for λ versus ε when Ω is the unit disk with a concentric circular patch of radius ε centered at the origin. The solid curve is the eigenvalue λ as obtained from the exact transcendental relation (2.28). The parameter values are $m_b = 2$ and $m_+ = 1$.

The first positive root of (2.28) is the positive principle eigenvalue of (2.1). For $\varepsilon \to 0$, we expand this root as

$$\lambda = \mu_0\nu + \mu_1\nu^2 + \cdots\,, \qquad \nu \equiv -1/\log\varepsilon\,. \tag{2.29a}$$

By using well-known asymptotic formulae for the Bessel and Modified Bessel functions of small argument, we substitute (2.29a) into (2.28), and equate coefficients

in powers of ν to obtain that

$$\mu_0 = \frac{2}{m_+}\left[1 - \frac{m_+}{m_b}\right], \qquad \mu_1 = \frac{\mu_0}{2}. \tag{2.29b}$$

For the special case where Ω is the unit disk containing a circular patch of radius ε, we need only substitute $|\Omega| = \pi$ and $R(0;0) = -3/(8\pi)$, obtained from (B.1b) of Appendix B, into (2.26a) of Principal Result 2.1. The resulting two-term expansion for λ agrees with (2.29). In Fig. 2 we show a very favorable comparison between the two-term expansion (2.29) for λ and the corresponding exact result obtained by finding the first positive root of (2.28) numerically.

2.2. **A Single Boundary Patch.** Next, we let the center x_0 of the circular patch be on $\partial\Omega$. We assume that $\partial\Omega$ is piecewise differentiable, but allow for $\partial\Omega$ to have corners with nonzero contact angle. The boundary patch $\Omega_{\varepsilon_0} \equiv \{x \,|\, |x - x_0| \le \varepsilon\rho_0 \cap \Omega\}$ with $x_0 \in \partial\Omega$ is the portion of a circular disk of radius $\varepsilon\rho_0$ that is strictly contained within Ω. Here $\rho_0 = \mathcal{O}(1)$ is introduced in order to construct a boundary patch that has the same area as an interior patch. As shown in §4.1 below, this then enables us to compare the persistence threshold under a given fixed $\int_\Omega m\,dx$ for both the boundary and interior patch cases.

In the limit $\varepsilon \to 0$, and for $x - x_0 = \mathcal{O}(\varepsilon)$, we define $\pi\alpha_0$ to be angular fraction of the circular patch that is contained within Ω. More specifically, $\alpha_0 = 1$ whenever x_0 is at a smooth point of $\partial\Omega$, and $\alpha_0 = 1/2$ when x_0 is at a $\pi/2$ corner of $\partial\Omega$. The eigenvalue problem associated with this boundary patch is

$$\Delta\phi + \lambda\, m_\varepsilon(x)\phi = 0\,, \quad x \in \Omega; \qquad \partial_n\phi = 0\,, \quad x \in \partial\Omega\,; \qquad \int_\Omega \phi^2\,dx = 1\,, \tag{2.30a}$$

where $m_\varepsilon(x)$ is defined as

$$m_\varepsilon(x) = \begin{cases} m_+/\varepsilon^2\,, & x \in \Omega_{\varepsilon_0}\,, \\ -m_b\,, & x \in \Omega\backslash\Omega_{\varepsilon_0}\,. \end{cases} \tag{2.30b}$$

The condition $\int_\Omega m\,dx < 0$ is asymptotically equivalent when $\varepsilon \to 0$ to

$$\int_\Omega m\,dx = -m_b|\Omega| + \frac{\alpha_0\pi}{2}\left(m_+\rho_0^2\right) + \mathcal{O}(\varepsilon^2) < 0\,. \tag{2.31}$$

We assume that this condition on $\int_\Omega m\,dx$ holds. Since the asymptotic calculation of λ for a boundary patch is similar to that for the interior patch case, we mainly highlight the new features that are required in the analysis.

We first expand λ as in (2.3) in terms of $\nu = -1/\log\varepsilon$. In the outer region, defined for $|x - x_0| \gg \mathcal{O}(\varepsilon)$, we expand the outer solution as in (2.4) to obtain that ϕ_0 is a constant, and that ϕ_1 and ϕ_2 satisfy (2.5a) and (2.5b) in Ω, respectively, with $\partial_n\phi_k = 0$ for $x \in \partial\Omega\backslash\{x_0\}$ for $k = 1, 2$.

Since the expansion of the inner solution is again in powers of $\nu = -1/\log\varepsilon$ as in (2.8), we can neglect to any power of ν the effect of the curvature of the domain boundary near $x = x_0$, provided that this curvature is finite. Consequently, when x_0 is at a smooth point of $\partial\Omega$, we can approximate $\partial\Omega$ near $x = x_0$ by the tangent line to $\partial\Omega$ through $x = x_0$. Alternatively, when x_0 is at corner point of $\partial\Omega$, the inner region is the angular wedge of angle $\pi\alpha_0$ bounded by the intersection of the one-sided tangent lines to $\partial\Omega$ at $x = x_0$. We then introduce the inner variable $y = \varepsilon^{-1}(x - x_0)$ so that the inner region is the angular wedge $\beta_0 < \arg y \le \alpha_0\pi + \beta_0$ for some β_0. The favorable habitat is the circular patch $|y| \le \rho_0$ that lies within this wedge. Since the no-flux boundary conditions $\partial_n\psi = 0$ holds on the two sides of the wedge, we look for a local radially symmetric inner solution within the angular wedge.

Therefore, in the inner region, we expand the inner solution as in (2.8) and obtain that ψ_0 is a constant, and that ψ_k for $k = 1, 2$ satisfies

$$\Delta\psi_k = \begin{cases} \mathcal{F}_k\,, & |y| \le \rho_0\,, \quad \beta_0 \le \arg y \le \pi\alpha_0 + \beta_0\,, \\ 0\,, & |y| \ge \rho_0\,, \quad \beta_0 \le \arg y \le \pi\alpha_0 + \beta_0\,. \end{cases} \tag{2.32}$$

Here $\mathcal{F}_k$ for $k = 1, 2$ are defined in (2.9b). The solution for ψ_1, with $\rho = |y|$, is

$$\psi_1 = \begin{cases} A_1\left(\dfrac{\rho^2}{2\rho_0^2}\right) + \bar{\psi}_1\,, & 0 \le \rho \le \rho_0\,, \quad \beta_0 \le \arg y \le \pi\alpha_0 + \beta_0\,, \\ A_1\log\left(\dfrac{\rho}{\rho_0}\right) + \dfrac{A_1}{2} + \bar{\psi}_1\,, & \rho \ge \rho_0\,, \quad \beta_0 \le \arg y \le \pi\alpha_0 + \beta_0\,, \end{cases} \tag{2.33}$$

where $\bar{\psi}_1$ is an unknown constant and $A_1 = \mathcal{F}_1\rho_0^2/2$. For ψ_2, we obtain that $\psi_2 \sim A_2\log\rho$ as $\rho \to \infty$. The calculation of A_2 proceeds exactly as in (2.11b) to obtain

$$A_1 = -\frac{\mu_0}{2}m_+\rho_0^2\psi_0\,, \qquad A_2 = \frac{A_1}{\psi_0}\left(\frac{A_1}{4} + \bar{\psi}_1 + \frac{\mu_1}{\mu_0}\psi_0\right)\,. \tag{2.34}$$

The matching condition between the outer solution as $x \to x_0$ and the inner solution for $|y| = \varepsilon^{-1}|x - x_0| \to \infty$ is given by (2.12). Upon using (2.33) for ψ_1 when $\rho \gg 1$, together with $\psi_2 \sim A_2\log\rho$ for $\rho \gg 1$, we obtain that (2.12) becomes

$$\begin{aligned} \phi_0 + \nu\phi_1 + \nu^2\phi_2 + \cdots \sim \psi_0 + A_1 + \nu\Big(A_1\log|x - x_0| - A_1\log\rho_0 + \frac{A_1}{2} + \bar{\psi}_1 + A_2\Big) \\ + \nu^2\left(A_2\log|x - x_0| + \mathcal{O}(1)\right)\,. \end{aligned} \tag{2.35}$$

The leading order matching condition from (2.35) is that

$$\phi_0 = \psi_0 + A_1\,. \tag{2.36}$$

From the $\mathcal{O}(\nu)$ terms in (2.35) and (2.5a), we obtain that ϕ_1 satisfies

$$\Delta\phi_1 = \mu_0 m_b \phi_0\,, \quad x\in\Omega\,; \qquad \partial_n\phi_1 = 0\,, \quad x\in\partial\Omega\backslash\{x_0\}\,; \qquad \int_\Omega \phi_1\,dx = 0\,, \tag{2.37a}$$

$$\phi_1 \sim A_1\log|x-x_0| - A_1\log\rho_0 + \frac{A_1}{2} + \bar{\psi}_1 + A_2\,, \quad \text{as} \quad x\to x_0\,. \tag{2.37b}$$

Moreover, from the $\mathcal{O}(\nu^2)$ terms in (2.35) and the problem for ϕ_2 (2.5b), we get that ϕ_2 satisfies

$$\Delta\phi_2 = \mu_1 m_b\phi_0 + \mu_0 m_b\phi_1\,, \quad x\in\Omega\,; \qquad \partial_n\phi_2 = 0\,, \quad x\in\partial\Omega\backslash\{x_0\}\,; \tag{2.38a}$$

$$\int_\Omega \left(\phi_1^2 + 2\phi_0\phi_2\right)\,dx = 0; \qquad \phi_2 \sim A_2\log|x-x_0| + \mathcal{O}(1)\,, \quad \text{as} \quad x\to x_0\,. \tag{2.38b}$$

Next, we apply the divergence theorem to (2.37) over $\Omega\backslash\Omega_\sigma$, where Ω_σ is a wedge of angle $\pi\alpha_0$ and small radius $\sigma\ll 1$ centered at $x_0\in\partial\Omega$. Imposing the singularity condition (2.37b) on $|x-x_0|=\sigma$ and taking the limit $\sigma\to 0$, we readily derive that

$$\mu_0 m_b|\Omega|\phi_0 = -\alpha_0\pi A_1\,. \tag{2.39}$$

In a similar way, the divergence theorem applied to (2.38), and noting that $\int_\Omega \phi_1\,dx = 0$, determines A_2 as

$$\mu_1 m_b|\Omega|\phi_0 = -\alpha_0\pi A_2\,. \tag{2.40}$$

Therefore, we conclude from (2.39) and (2.40) that $A_2/A_1 = \mu_1/\mu_0$, which yields $\bar{\psi}_1 = -A_1/4$ from the equation for A_2 in (2.34). Then, by combining (2.36), (2.34) for A_1, and (2.39), we readily obtain that

$$\psi_0 = \frac{2m_b|\Omega|}{\alpha_0\pi m_+\rho_0^2}\phi_0\,, \qquad \mu_0 = \frac{2}{m_+\rho_0^2}\left[1 - \frac{\alpha_0\pi m_+\rho_0^2}{2m_b|\Omega|}\right]\,. \tag{2.41}$$

Since $\int_\Omega m\,dx < 0$ from (2.31), it follows that $\mu_0 > 0$ in (2.41).

To solve (2.37), we introduce the surface Neumann Green's function $G_s(x;x_0)$, defined as the unique solution of

$$\Delta G_s = \frac{1}{|\Omega|}\,, \quad x\in\Omega\,; \qquad \partial_n G_s = 0\,, \qquad x\in\partial\Omega\backslash\{x_0\}\,; \qquad \int_\Omega G_s\,dx = 0\,, \tag{2.42a}$$

$$G_s(x;x_0) \sim -\frac{1}{\alpha_0\pi}\log|x-x_0| + R_s(x_0;x_0)\,, \quad \text{as} \quad x\to x_0\in\partial\Omega\,. \tag{2.42b}$$

Here $|\Omega|$ is the area of Ω, and $R_s(x_0;x_0)$ is the regular part of the surface Neumann Green's function at $x=x_0$. Then, the solution to (2.37) is

$$\phi_1 = -\alpha_0\pi A_1 G_s(x;x_0)\,. \tag{2.43}$$

By expanding ϕ_1 as $x\to x_0$ using (2.42b), we equate the resulting nonsingular part of ϕ_1 as $x\to x_0$ with that in (2.37b) to obtain

$$-\alpha_0\pi A_1 R_s(x_0;x_0) = -A_1\log\rho_0 + \frac{A_1}{2} + \bar{\psi}_1 + A_2\,. \tag{2.44}$$

We then substitute $\bar{\psi}_1 = -A_1/4$ and $A_2/A_1 = \mu_1/\mu_0$ into (2.44), and solve for μ_1 to get

$$\mu_1 = \mu_0 \left[\log \rho_0 - \frac{1}{4} - \alpha_0 \pi R_s(x_0; x_0) \right] . \tag{2.45}$$

We summarize our result as follows:

Principal Result 2.2: *In the limit of small boundary patch radius, $\varepsilon \to 0$, a two-term asymptotic expansion for the positive principal eigenvalue λ of (2.30) in terms of $\nu = -1/\log \varepsilon$ is*

$$\begin{aligned} \lambda &= \mu_0 \nu - \mu_0 \nu^2 \left[\frac{1}{4} + \alpha_0 \pi R_s(x_0; x_0) - \log \rho_0 \right] + \mathcal{O}(\nu^3) \, ; \\ \mu_0 &\equiv \frac{2}{m_+ \rho_0^2} \left[1 - \frac{\alpha_0 \pi m_+ \rho_0^2}{2|\Omega| m_b} \right] . \end{aligned} \tag{2.46a}$$

A two-term asymptotic expansion for the corresponding eigenfunction in the outer region $|x - x_0| \gg \mathcal{O}(\varepsilon)$ is

$$\phi \sim \phi_0 \left(1 + \nu \mu_0 m_b |\Omega| G_s(x; x_0) \right) . \tag{2.46b}$$

Here $G_s(x; x_0)$ is the surface Neumann Green's function of (2.42) with regular part $R_s(x_0; x_0)$.

The implication of Principal Results 2.1 and 2.2 for the determination of the persistence threshold is discussed in §4.1.

3. The Persistence Threshold for Multiple Patches.

In this section we generalize the analysis of §2 to treat the case of an arbitrary but fixed number n of circular patches, each of which is centered either inside Ω or on $\partial\Omega$. To this end, we asymptotically calculate the positive principal eigenvalue of

$$\Delta \phi + \lambda \, m_\varepsilon(x) \phi = 0 \, , \quad x \in \Omega; \qquad \partial_n \phi = 0 \, , \quad x \in \partial\Omega \, ; \qquad \int_\Omega \phi^2 \, dx = 1 \, , \tag{3.1a}$$

where the growth rate function $m_\varepsilon(x)$ is defined by

$$m_\varepsilon(x) = \begin{cases} m_j/\varepsilon^2 \, , & x \in \Omega_{\varepsilon_j} \, , \quad j = 1, \ldots, n \, , \\ -m_b \, , & x \in \Omega \backslash \bigcup_{j=1}^n \Omega_{\varepsilon_j} \, . \end{cases} \tag{3.1b}$$

Here $\Omega_{\varepsilon_j} \equiv \{ x \, | \, |x - x_j| \le \varepsilon \rho_j \cap \Omega \}$, so that the patches Ω_{ε_j} are the portions of the circular disks of radius $\varepsilon \rho_j$ that are strictly inside Ω. The constant m_j is the local growth rate of the j^{th} patch, with $m_j > 0$ for a favorable habitat and $m_j < 0$ for an unfavorable habitat. The constant $m_b > 0$ is the background bulk decay rate for the unfavorable habitat. In terms of this patch arrangement, the condition $\int_\Omega m \, dx < 0$ is asymptotically equivalent for $\varepsilon \to 0$ to

$$\int_\Omega m \, dx = -m_b |\Omega| + \frac{\pi}{2} \sum_{j=1}^n \alpha_j m_j \rho_j^2 + \mathcal{O}(\varepsilon^2) < 0 \, . \tag{3.2}$$

We assume that the parameters are chosen so that this condition holds. The patches are assumed to be well-separated in the sense mentioned in §1. The parameters in the growth rate are the centers $x_1,\dots,x_n$ of the circular patches, their radii $\varepsilon\rho_1,\dots,\varepsilon\rho_n$, the local growth rates $m_1,\dots,m_n$, the angular fractions $\pi\alpha_1,\dots,\pi\alpha_n$ of the circular patches that are contained in Ω, and the constant bulk growth rate m_b. Recall that $\alpha_j=2$ whenever $x_j\in\Omega$, $\alpha_j=1$ when $x_j\in\partial\Omega$ and x_j is a point where $\partial\Omega$ is smooth, and $\alpha_j=1/2$ when $x_j\in\partial\Omega$ is at a $\pi/2$ corner of $\partial\Omega$, etc.

To asymptotically analyze (3.1) we must incorporate both the Neumann Green's function and the surface Neumann Green's function. As such, we define a generalized modified Green's function $G_m(x;x_j)$ by

$$G_m(x;x_j)\equiv\begin{cases} G(x;x_j)\,, & x_j\in\Omega\,,\\ G_s(x;x_j)\,, & x_j\in\partial\Omega\,. \end{cases} \tag{3.3a}$$

Here $G(x;x_j)$ is the Neumann Green's function of (2.19), and $G_s(x;x_j)$ is the surface Neumann Green's function of (2.42). Therefore, the local behavior of $G_m(x;x_j)$ is

$$\begin{aligned} &G_m(x;x_j)\sim-\frac{1}{\alpha_j\pi}\log|x-x_j|+R_m(x_j;x_j)\,,\quad \text{as}\quad x\to x_j\,,\\ &R_m(x_j;x_j)\equiv\begin{cases} R(x_j;x_j)\,, & x_j\in\Omega\,,\\ R_s(x_j;x_j)\,, & x_j\in\partial\Omega\,. \end{cases} \end{aligned} \tag{3.3b}$$

Here $R(x_j;x_j)$ and $R_s(x_j;x_j)$ are the regular part of the Neumann Green's function (2.19) and the surface Neumann Green's function (2.42), respectively.

We now derive a two-term expansion for the positive principal eigenvalue of (3.1). We expand λ as in (2.3), and we expand the outer representation for the eigenfunction ϕ as in (2.4). Upon substituting (2.3) and (2.4) into (3.1), we obtain that $\phi_0=|\Omega|^{-1/2}$ is a constant, and that ϕ_1 and ϕ_2 satisfy

$$\Delta\phi_1=\mu_0 m_b\phi_0\,,\quad x\in\Omega\backslash\Omega^I\,;\qquad \partial_n\phi_1=0\,,\quad x\in\partial\Omega\backslash\Omega^B\,;\qquad \int_\Omega\phi_1\,dx=0\,, \tag{3.4a}$$

$$\Delta\phi_2=\mu_1 m_b\phi_0+\mu_0 m_b\phi_1\,,\quad x\in\Omega\backslash\Omega^I\,;\qquad \partial_n\phi_2=0\,,\quad x\in\partial\Omega\backslash\Omega^B\,;\qquad \int_\Omega\left(\phi_1^2+2\phi_0\phi_2\right)\,dx=0\,. \tag{3.4b}$$

In (3.4), we recall from §1 that $\Omega^I\equiv\{x_1,\dots,x_n\}\cap\Omega$ denotes the set of the centers of the interior patches, while $\Omega^B\equiv\{x_1,\dots,x_n\}\cap\partial\Omega$ denotes the set of the centers of the boundary patches.

In the inner region, near the j^{th} patch we introduce the local variables $y=\varepsilon^{-1}(x-x_j)$ and $\psi(y)=\phi(x_j+\varepsilon y)$. We then expand ψ for $y=\mathcal{O}(1)$ by

$$\psi\sim\psi_{0j}+\nu\psi_{1j}+\nu^2\psi_{2j}+\cdots\,, \tag{3.5}$$

where ψ_{0j} is a constant to be determined. For an interior patch with $x_j \in \Omega^I$, we obtain that ψ_{kj} for $k = 1, 2$ satisfy

$$\Delta\psi_{kj} = \begin{cases} \mathcal{F}_{kj}\,, & |y| \le \rho_j\,, \\ 0\,, & |y| \ge \rho_j\,, \end{cases} \tag{3.6}$$

where $\mathcal{F}_{1j} = -\mu_0 m_j \psi_{0j}$ and $\mathcal{F}_{2j} = -\mu_0 m_j \psi_{1j} - \mu_1 m_j \psi_{0j}$. The solution for ψ_{1j}, with $\rho = |y|$, is

$$\psi_{1j} = \begin{cases} A_{1j}\left(\frac{\rho^2}{2\rho_j^2}\right) + \bar{\psi}_{1j}\,, & 0 \le \rho \le \rho_j\,, \\ A_{1j}\log\left(\frac{\rho}{\rho_j}\right) + \frac{A_{1j}}{2} + \bar{\psi}_{1j}\,, & \rho \ge \rho_j\,, \end{cases} \tag{3.7}$$

where $\bar{\psi}_{1j}$ is an unknown constant. In addition, $\psi_{2j} \sim A_{2j}\log\rho$ as $\rho \to \infty$. The divergence theorem is used to calculate A_{1j} and A_{2j} from (3.6), as was done in §2, to obtain

$$A_{1j} = -\frac{\mu_0}{2} m_j \rho_j^2 \psi_{0j}\,, \qquad A_{2j} = \frac{A_{1j}}{\psi_{0j}}\left(\frac{A_{1j}}{4} + \bar{\psi}_{1j} + \frac{\mu_1}{\mu_0}\psi_{0j}\right). \tag{3.8}$$

For a boundary patch, for which $x_j \in \Omega^B$, then (3.6) holds in the wedge $\beta_j < \arg(y) < \beta_j + \pi\alpha_j$, for some β_j and $0 < \alpha_j < 2$. For this boundary case, the constants A_{1j} and A_{2j} are also given by (3.8).

The matching condition between the outer solution as $x \to x_j$ and the inner solution as $|y| = \varepsilon^{-1}|x - x_j| \to \infty$ is

$$\begin{aligned} \phi_0 + \nu\phi_1 + \nu^2\phi_2 + \cdots \sim\ & \psi_{0j} + A_{1j} \\ & + \nu\left(A_{1j}\log|x - x_j| - A_{1j}\log\rho_j + \frac{A_{1j}}{2} + \bar{\psi}_{1j} + A_{2j}\right) \\ & + \nu^2\left(A_{2j}\log|x - x_j| + \mathcal{O}(1)\right). \end{aligned} \tag{3.9}$$

The leading-order matching condition from (3.9) yields

$$\phi_0 = \psi_{0j} + A_{1j}\,, \qquad j = 1, \ldots, n\,. \tag{3.10}$$

From the $\mathcal{O}(\nu)$ terms in (3.9), we obtain that ϕ_1 has the following singular behavior as $x \to x_j$

$$\phi_1 \sim A_{1j}\log|x - x_j| - A_{1j}\log\rho_j + \frac{A_{1j}}{2} + \bar{\psi}_{1j} + A_{2j}\,, \quad \text{as} \quad x \to x_j\,. \tag{3.11}$$

In addition, from the $\mathcal{O}(\nu^2)$ terms in (3.9), we conclude that

$$\phi_2 \sim A_{2j}\log|x - x_j| + \mathcal{O}(1)\,, \quad \text{as} \quad x \to x_j\,. \tag{3.12}$$

Next, by using the divergence theorem on the solution ϕ_1 to (3.4a) with singular behavior (3.11) we obtain

$$\mu_0 m_b |\Omega|\phi_0 = -\pi\sum_{j=1}^{n}\alpha_j A_{1j}\,. \tag{3.13}$$

Similarly, the divergence theorem applied to (3.4b) with singular behavior (3.12), and noting $\int_\Omega \phi_1\,dx = 0$, yields

$$\mu_1 m_b|\Omega|\phi_0 = -\pi\sum_{j=1}^{n}\alpha_j A_{2j}\,. \tag{3.14}$$

By combining (3.10) and (3.8) for A_{1j}, we obtain that

$$\psi_{0j} = \frac{2\phi_0}{2-m_j\rho_j^2\mu_0}\,, \qquad A_{1j} = -\frac{m_j\rho_j^2\mu_0\phi_0}{2-m_j\rho_j^2\mu_0}\,, \qquad j=1,\dots,n\,. \tag{3.15}$$

From (3.13), together with (3.15) for A_{1j}, we obtain that the leading-order eigenvalue correction μ_0 is a root of the nonlinear algebraic equation

$$\frac{m_b|\Omega|}{\pi} = \sum_{j=1}^{n}\frac{\alpha_j m_j\rho_j^2}{2-m_j\rho_j^2\mu_0}\,. \tag{3.16}$$

The properties of the roots to (3.16) are studied below following Principal Result 3.1.

Next, we write the solution ϕ_1 to (3.4a) with singular behavior (3.11) in terms of the modified Green's function $G_m(x;x_j)$ of (3.3) as

$$\phi_1 = -\pi\sum_{i=1}^{n}\alpha_i A_{1i}G_m(x;x_i)\,. \tag{3.17}$$

Then, by expanding ϕ_1 as $x\to x_j$ and by using (3.3b) for the local behavior of $G_m(x;x_j)$, we obtain that

$$\phi_1 \sim A_{1j}\log|x-x_j| - \pi\alpha_j A_{1j}R_{mjj} + B_j\,, \quad \text{as} \quad x\to x_j; \quad B_j \equiv -\pi\sum_{\substack{i=1\\ i\neq j}}^{n}\alpha_i A_{1i}G_{mji}\,, \tag{3.18}$$

where $G_{mji}\equiv G_m(x_j;x_i)$. The requirement that the nonsingular terms in (3.11) and (3.18) agree yields the constraints

$$-\pi\alpha_j A_{1j}R_{mjj} + B_j = -A_{1j}\log\rho_j + \frac{A_{1j}}{2} + \bar{\psi}_{1j} + A_{2j}\,, \qquad j=1,\dots,n\,, \tag{3.19}$$

where $R_{mjj}\equiv R_m(x_j;x_j)$ is the regular part of the generalized modified Green's function as defined in (3.3b).

Next, we combine (3.8), (3.15), and (3.19) to isolate A_{2j}. Then, μ_1 is determined from (3.14). To do so, we first solve (3.19) for $\bar{\psi}_{1j}$. Upon substituting the resulting expression for $\bar{\psi}_{1j}$, together with $A_{1j}/\psi_{0j} = -m_j\rho_j^2\mu_0/2$ from (3.8), into (3.8) for A_{2j}, we obtain for each $j=1,\dots,n$ that

$$A_{2j} = -\frac{m_j\rho_j^2\mu_0}{2}\left(-\frac{A_{1j}}{4} - \pi\alpha_j A_{1j}R_{mjj} + B_j + A_{1j}\log\rho_j - A_{2j}\right) + \frac{\mu_1}{\mu_0}A_{1j}\,. \tag{3.20}$$

Upon solving this equation for A_{2j}, and using (3.18) for B_j, we isolate the product $\alpha_j A_{2j}$ as

$$\alpha_j A_{2j} = -\frac{m_j\rho_j^2\mu_0}{\left(2-m_j\rho_j^2\mu_0\right)}\left[\begin{array}{l} -\pi\alpha_j^2 A_{1j}R_{mjj} + \alpha_j A_{1j}\log\rho_j \\ -\dfrac{\alpha_j A_{1j}}{4} - \pi\displaystyle\sum_{\substack{i=1\\ i\neq j}}^{n}\alpha_i\alpha_j A_{1i}G_{mji} \end{array}\right] + \frac{\mu_1}{\mu_0}\Big(\frac{2A_{1j}\alpha_j}{2-m_j\rho_j^2\mu_0}\Big). \tag{3.21}$$

Next, it is convenient to introduce a new variable κ_j and to rewrite A_{1j} of (3.15) in terms of this variable as

$$\kappa_j \equiv \frac{\sqrt{\alpha_j}m_j\rho_j^2}{2-m_j\rho_j^2\mu_0}\,, \qquad A_{1j} = -\frac{\mu_0\kappa_j}{\sqrt{\alpha_j}}\phi_0\,, \qquad j=1,\ldots,n\,. \tag{3.22}$$

It is also convenient to introduce the symmetric $n\times n$ Green's matrix $\mathcal{G}_m$, and the diagonal matrix $\mathcal{P}$, with matrix entries $\mathcal{G}_{mij}$ and $\mathcal{P}_{ij}$ defined by

$$\begin{aligned} &\mathcal{G}_{mij} = \sqrt{\alpha_i\alpha_j}G_{mij}\,, \quad i\neq j\,; \qquad \mathcal{G}_{mjj} = \alpha_j R_{mjj}\,; \\ &\mathcal{P}_{ij} = 0\,, \quad i\neq j\,; \qquad \mathcal{P}_{jj} = \log\rho_j\,. \end{aligned} \tag{3.23}$$

In terms of κ_j, $\mathcal{G}_m$, $\mathcal{P}$, and the vector $\kappa=(\kappa_1,\ldots,\kappa_n)^t$, (3.21) readily reduces to

$$\alpha_j A_{2j} = -\mu_0^2\phi_0\kappa_j\left[\pi\left(\mathcal{G}_m\kappa\right)_j - \left(\mathcal{P}\kappa\right)_j + \frac{\kappa_j}{4}\right] - \frac{2\mu_1\kappa_j^2}{m_j\rho_j^2}\phi_0\,, \tag{3.24}$$

where $\left(\mathcal{P}\kappa\right)_j$ and $\left(\mathcal{G}_m\kappa\right)_j$ denote the j^{th} component of the vectors $\mathcal{P}\kappa$ and $\mathcal{G}_m\kappa$, respectively.

Finally, we substitute (3.24) into (3.14), and solve the resulting expression for μ_1 to obtain

$$\mu_1\left[\frac{m_b|\Omega|}{\pi} - \sum_{j=1}^{n}\frac{2\kappa_j^2}{m_j\rho_j^2}\right] = \mu_0^2\left[\kappa^t\left(\pi\mathcal{G}_m-\mathcal{P}\right)\kappa + \frac{1}{4}\kappa^t\kappa\right]. \tag{3.25}$$

The left-hand side of (3.25) is simplified by using the equation (3.16) for μ_0 to obtain

$$\begin{aligned} \frac{m_b|\Omega|}{\pi} - \sum_{j=1}^{n}\frac{2\kappa_j^2}{m_j\rho_j^2} &= \sum_{j=1}^{n}\frac{\alpha_j}{\left(2-m_j\rho_j^2\mu_0\right)}\left[m_j\rho_j^2 - \frac{2m_j\rho_j^2}{\left(2-m_j\rho_j^2\mu_0\right)}\right], \\ &= -\sum_{j=1}^{n}\frac{\alpha_j}{\left(2-m_j\rho_j^2\mu_0\right)}\left[\frac{\mu_0 m_j^2\rho_j^4}{\left(2-m_j\rho_j^2\mu_0\right)}\right] = -\mu_0\kappa^t\kappa\,. \end{aligned} \tag{3.26}$$

This determines μ_1 from (3.25) in terms of a Rayleigh-type quotient. We summarize our result as follows:

Principal Result 3.1: *In the limit of small patch radius, $\varepsilon\to 0$, the positive principal eigenvalue λ of (3.1) has the following two-term asymptotic expansion in terms of the logarithmic gauge function $\nu=-1/\log\varepsilon$:*

$$\lambda = \mu_0\nu - \mu_0\nu^2\left(\frac{\kappa^t\left(\pi\mathcal{G}_m-\mathcal{P}\right)\kappa}{\kappa^t\kappa} + \frac{1}{4}\right) + \mathcal{O}(\nu^3)\,. \tag{3.27}$$

Here $\mu_0 > 0$ is the first positive root of $\mathcal{B}(\mu_0) = 0$, where $\mathcal{B}(\mu_0)$ is defined by

$$\mathcal{B}(\mu_0) \equiv -m_b|\Omega| + \pi \sum_{j=1}^{n} \frac{\alpha_j m_j \rho_j^2}{2 - m_j \rho_j^2 \mu_0} \,. \tag{3.28}$$

In (3.27), $\kappa = (\kappa_1, \ldots, \kappa_n)^t$, where κ_j is defined in (3.22), while $\mathcal{G}_m$ and $\mathcal{P}$ are the $n \times n$ matrices as defined in (3.23). In addition, a two-term expansion for the outer solution is given by

$$\phi \sim \phi_0 \Big(1 + \nu \pi \mu_0 \sum_{j=1}^{n} \sqrt{\alpha_j} \kappa_j G_m(x; x_j) \Big) \,. \tag{3.29}$$

Next, we show the existence of a unique root μ_0 to (3.28) on a certain interval with $\mu_0 > 0$ to be determined. Since $\int_\Omega m \, dx < 0$ from (3.2), it follows that $\mathcal{B}(0) < 0$ from (3.28). In addition, $\mathcal{B}(\mu_0) \to +\infty$ as $\mu_0 \to 2/(m_J \rho_J^2)$ from below, where $m_J \rho_J^2$ is defined by

$$m_J \rho_J^2 = \max_{m_j > 0} \{ m_j \rho_j^2 \, | \, j = 1, \ldots, n \} \,. \tag{3.30}$$

There must be at least one j for which $m_j > 0$, so that (3.30) is attained at some $j = J$. Moreover, (3.28) readily yields that $\mathcal{B}'(\mu_0) > 0$ on $0 < \mu_0 < 2/(m_J \rho_J^2)$. Therefore, there exists a unique root $\mu_0 = \mu_0^\star$ on $0 < \mu_0 < 2/(m_J \rho_J^2)$ to $\mathcal{B}(\mu_0) = 0$. The corresponding leading-order eigenfunction in the inner region, ψ_{0j}, satisfies $\psi_{0j} > 0$ from (3.15). Therefore, $\mu_0^\star$ is the leading-order term in the asymptotic expansion of the positive principal eigenvalue of (3.1).

Although the required root to (3.28) must in general be computed numerically, there are two special cases where it can be found analytically. In the symmetric case where $m_j = m_c$ and $\rho_j = \rho_c$ for $j = 1, \ldots, n$, then, the root of (3.28) is simply

$$\mu_0 = \frac{2}{m_c \rho_c^2} \left[1 - \frac{\pi \alpha_s m_c \rho_c^2}{2 m_b |\Omega|} \right] \,, \qquad \alpha_s \equiv \sum_{j=1}^{n} \alpha_j \,. \tag{3.31}$$

In addition, if there are only two types of patches, such as $m_j \rho_j^2 = m_c \rho_c^2$ for $j = 1, \ldots, n-1$ and $m_n \rho_n^2$, then (3.28) reduces to a quadratic equation for μ_0, which can be solved explicitly.

Finally, we remark that our asymptotic analysis leading to Principal Result 3.1 has two limitations. Firstly, it is valid only when all interior or boundary patches are well-separated in the sense that $|x_i - x_j| \gg \mathcal{O}(\varepsilon)$ for $i \neq j$. Therefore, if we allow the distance between any two interior patches to depend on ε, our analysis is not valid for the case where this distance is $\mathcal{O}(\varepsilon)$. The case of two interior patches with an $\mathcal{O}(\varepsilon)$ center-to-center separation leads to an inner patch problem that does not appear to be tractable analytically. In addition, in our analysis we required that all interior patches are not too close to the boundary, in the sense that $|x - x_j| \gg \mathcal{O}(\varepsilon)$ for $x_j \in \Omega^I$ and $x \in \partial\Omega$.

4. **The Effect of Fragmentation and Location of Resources on Species Persistence.** In this section, the formulae derived in §2 and §3 for the persistence threshold, $\lambda(\varepsilon)$, are used to determine the optimal strategy for distributing a fixed quantity of resources in some domain where favorable and unfavorable patches may already be present. The constraint that the resources being distributed are fixed is expressed mathematically by

$$-m_b|\Omega| + \frac{\pi}{2}\sum_{j=1}^{n}\alpha_j m_j \rho_j^2 + \mathcal{O}(\varepsilon^2) = \int_\Omega m\,dx = -K\,, \tag{4.1}$$

where $K > 0$ is kept constant as m_b, or α_j, m_j, and ρ_j, for $j = 1, \ldots, n$ are varied.

4.1. **The Persistence Threshold for One Patch.** We first consider the case of one favorable habitat. For an interior patch of area $\pi\varepsilon^2$, we recall that λ is given in (2.26a) of Principal Result 2.1. For a boundary patch of the same area, we must set $\pi\alpha_0\varepsilon^2\rho_0^2/2 = \pi\varepsilon^2$ in (2.46a) of Principal Result 2.2. Thus, $\rho_0 = \sqrt{2/\alpha_0}$, so that (2.46a) becomes

$$\begin{aligned} &\lambda = \mu_0\nu - \mu_0\nu^2\left[\frac{1}{4} + \alpha_0\pi R_s(x_0;x_0) - \frac{1}{2}\log\left(\frac{2}{\alpha_0}\right)\right] + \mathcal{O}(\nu^3)\,; \\ &\mu_0 \equiv \frac{\alpha_0}{m_+}\left[1 - \frac{\pi m_+}{|\Omega| m_b}\right]\,. \end{aligned} \tag{4.2}$$

By comparing the leading-order $\mathcal{O}(\nu)$ terms in (4.2) and (2.26a), and noting that $\alpha_0 < 2$ for a boundary patch, we obtain the following main result:

Principal Result 4.1: *For a favorable habitat of area $\pi\varepsilon^2$, the positive principal eigenvalue λ is always smaller for a boundary patch than for an interior patch. For a domain boundary with corners, λ is minimized when the boundary patch is centered at the corner with the smallest corner contact angle $\pi\alpha_0$, as opposed to a patch on the smooth part of the boundary, only if $\alpha_0 < 1$. For a domain with smooth boundary, for which $\alpha_0 = 1$ for any $x_0 \in \partial\Omega$, then λ in (4.2) is minimized when the center x_0 of the boundary patch is located at the global maximum of the regular part $R_s(x_0;x_0)$ of the surface Neumann Green's function of (2.42) on $\partial\Omega$.*

We remark that the condition $\alpha_0 < 1$ in the second sentence of Principal Result 4.1 is necessary since one can readily construct a nonconvex domain with a boundary that has exactly one corner, with this corner being re-entrant, i.e. with corner contact angle larger than π. For a square, Principal Result 4.1 shows that the best choice for the favorable habitat is to concentrate resources near one of the four corners of the square. However, for a domain Ω with a smooth boundary $\partial\Omega$, it is not clear whether the maximization of $R_s(x_0;x_0)$, as required to minimize λ, has an obvious geometrical interpretation. When Ω is a smooth perturbation of the unit disk, we now examine whether the global maximum of $R_s(x_0;x_0)$ must necessarily

coincide with the global maximum of the curvature of the boundary. To do so, we require the following result of [20] determining the critical points of $R_s(x_0;x_0)$ for domains that are smooth perturbations of the unit disk:

Principal Result 4.2: [From [20]]: *Let Ω be a smooth perturbation of the unit disk with boundary given in terms of polar coordinates by*

$$r = r(\theta) = 1 + \delta\sigma(\theta)\,, \qquad \sigma(\theta) = \sum_{n=1}^{\infty} \left(a_n \cos(n\theta) + b_n \sin(n\theta)\right)\,, \qquad \delta \ll 1\,. \tag{4.3}$$

We assume that $\sigma(\theta)$ is 2π periodic and is at least C^2 smooth. Let $x_0 = x_0(\theta_0) = (r_0\cos\theta_0, r_0\sin\theta_0)$ be a point on the boundary where $r_0 = 1 + \delta\sigma(\theta_0)$. For $x \in \partial\Omega$ we define

$$\rho(\theta) \equiv R_s(x;x_0) \qquad \text{and} \qquad \rho(\theta_0) \equiv R_s(x_0;x_0)\,, \tag{4.4}$$

where $R_s(x;x_0)$ is the regular part of the Green's function defined by

$$R_s(x;x_0) = G_s(x;x_0) + \frac{1}{\pi}\log|x-x_0|\,, \quad x \in \Omega\,. \tag{4.5}$$

Then, for $\delta \ll 1$, $\rho'(\theta_0)$ satisfies

$$\rho'(\theta_0) = \frac{\delta}{\pi}\sum_{n=1}^{\infty}\left(n^2+n-2\right)\left(b_n\cos n\theta_0 - a_n \sin n\theta_0\right) + \mathcal{O}(\delta^2)\,. \tag{4.6}$$

The proof of this result was given in [20]. For the convenience of the reader this proof is given in Appendix A.

We first take the domain boundary to be $r = 1 + \delta\,\sin(2\theta)$, so that $\rho'(\theta_0) = 4\delta\pi^{-1}\cos(2\theta_0)$ from (4.6). In contrast, for $\delta \ll 1$, we calculate the curvature of the domain boundary as

$$\kappa(\theta) = \frac{r^2 + 2r_\theta^2 - r r_{\theta\theta}}{\left(r^2+r_\theta^2\right)^{3/2}} \sim 1 - \delta\left(\sigma + \sigma_{\theta\theta}\right) + \mathcal{O}(\delta^2)\,. \tag{4.7}$$

Therefore, for $r = 1 + \delta\,\sin(2\theta)$, we obtain that

$$\rho(\theta) = \frac{2\delta}{\pi}\sin(2\theta) + C\,, \qquad \kappa(\theta) = 1 + 3\delta\sin(2\theta)\,, \tag{4.8}$$

where C is some constant. For this example the global maxima of ρ and κ over $0 \le \theta < 2\pi$ do coincide, and are attained at $\theta = \pi/4$ and $\theta = 5\pi/4$.

Next, we use Principal Result 4.2 to establish the following result:

Principal Result 4.3: *The global maximum of $R_s(x_0,x_0)$ for $x_0 \in \partial\Omega$ does not necessarily coincide with the global maximum of the curvature $\kappa(\theta)$ of the boundary of a smooth perturbation of the unit disk. Consequently, for $\varepsilon \to 0$, the persistence threshold $\lambda(\varepsilon)$ from Principal Result 2.2 is not necessarily minimized when the center of the circular patch is located at the global maximum of the curvature of the smooth boundary $\partial\Omega$.*

To prove this result we take $a_2 = 1$, $b_3 = b$, with $a_n = 0$ for $n \neq 2$ and $b_n = 0$ for $n \neq 3$ in (4.3), so that

$$\sigma(\theta) = \cos(2\theta) + b\sin(3\theta)\,. \tag{4.9}$$

For $\delta \ll 1$, we use (4.7) for the curvature κ of $\partial\Omega$ to calculate

$$\kappa = 1 + \delta\left[3\cos(2\theta) + 8b\sin(3\theta)\right]\,, \qquad \kappa'(\theta) = -6\delta\left[\sin(2\theta) - 4b\cos(3\theta)\right]\,,$$
$$\kappa''(\theta) = -12\delta\left[\cos(2\theta) + 6b\sin(3\theta)\right]\,. \tag{4.10}$$

From (4.6) we calculate $\rho'(\theta)$ and its derivative as

$$\rho'(\theta) = -\frac{4\delta}{\pi}\left[\sin(2\theta) - \frac{5b}{2}\cos(3\theta)\right]\,, \qquad \rho''(\theta) = -\frac{8\delta}{\pi}\left[\cos(2\theta) + \frac{15b}{4}\sin(3\theta)\right]\,.$$

Therefore, in terms of an unknown constant C, we obtain that

$$\rho(\theta) = \frac{\delta}{\pi}\left[2\cos(2\theta) + \frac{10b}{3}\sin(3\theta)\right] + C\,. \tag{4.11}$$

We observe that $\theta = \pi/2$ and $\theta = 3\pi/2$ are the only two critical points shared by κ and ρ. The nature of these local extrema depend on the values of

$$\kappa''(\pi/2) = 12\delta(1+6b)\,, \quad \rho''(\pi/2) = \frac{8\delta}{\pi}\left(1 + \frac{15b}{4}\right)\,,$$
$$\kappa''(3\pi/2) = 12\delta(1-6b)\,, \quad \rho''(3\pi/2) = \frac{8\delta}{\pi}\left(1 - \frac{15b}{4}\right)\,.$$

Therefore, when b is chosen to satisfy $-4/15 < b < -1/6$, then κ has a local maximum while ρ has a local minimum at $\theta = \pi/2$. Similarly, for this range of b, κ has a local minimum while ρ has a local minimum at $\theta = 3\pi/2$.

Since the only critical points shared by κ and ρ are local minima of ρ, we conclude that the absolute maximum value of ρ occurs at a point where $\kappa'(\theta) \neq 0$. Therefore, in general, the point(s) where the absolute maximum value of ρ is attained do not coincide precisely with the maximum curvature of the boundary of the domain. In Fig. 3(a) we plot the domain boundary when $\delta = 0.1$ and $b = -1/5$. In Fig. 3(b) we plot $\rho(\theta) - C$ and $\kappa(\theta) - 1$ from (4.11) and (4.10), respectively, for $\delta = 0.1$ and $b = -1/5$ showing that the global maxima of ρ and $\kappa - 1$ occur at different, but nearby, locations.

In §3.3 of [20] a boundary element method (BEM) was formulated and implemented to numerically compute the regular part of the surface Neumann Green's function for an arbitrary bounded two-dimensional domain with smooth boundary. In Fig. 4 we show a very favorable comparison between full numerical results for $\rho(\theta)$ and the perturbation formula (4.11) for $\delta = 0.1$ and $b = -1/5$. The constant C in (4.11) was fitted to the full numerical results at $\theta = 0$. This figure provides a numerical validation of our perturbation result (4.11).

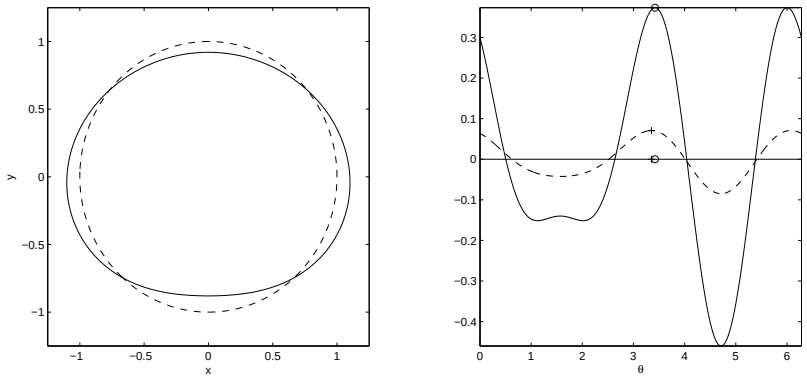

(a) perturbation of the unit disk (b) $\kappa(\theta)-1$ and $\rho(\theta)$ versus θ

FIGURE 3. Left figure: plot of the unit disk (dashed curve) and the perturbed unit disk (solid curve) with boundary $r = 1 + \delta\left(\cos(2\theta) + b\sin(3\theta)\right)$, where $\delta = 0.1$ and $b = -1/5$. Right figure: plot of the curvature perturbation $\kappa(\theta) - 1$ (solid curve) and the regular part $\rho(\theta)$ of the surface Neumann Green's function defined in (4.11) (dashed curve) with $C = 0$. The absolute maximum of $\kappa - 1$ and ρ are observed to occur at distinct, but nearby points, as indicated in the figure.

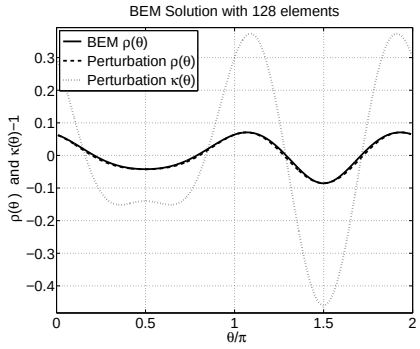

FIGURE 4. Plot of $\rho(\theta) \equiv R(x_0(\theta), x_0(\theta))$ computed by the BEM method (heavy solid curve) and the perturbation formula (4.11) (dashed curve) versus θ/π for a domain with boundary $r = 1 + \delta\left[\cos(2\theta) + b\sin(3\theta)\right]$ with $\delta = 0.1$ and $b = -1/5$. The curvature perturbation $\kappa(\theta) - 1$ is given by the dotted curve.

We conjecture that the relationship between the maximum of the boundary curvature and the location of the favorable habit that yields the minimum value of λ for a fixed $\int_\Omega m\, dx < 0$ is qualitatively similar to that for steady-state bubble-type transition-layer solutions for the Cahn-Hilliard model studied in [8]. In this latter

context, it was shown from variational considerations in [8] that the minimal-energy bubble solution attaches orthogonally to the domain boundary at two points, with the global maximum of the boundary curvature located somewhere between these two points. The transition layer associated with this bubble solution is the arc of a circle connecting these two attached boundary points. Similarly, for our boundary patch problem, we expect that for ε small but fixed, the maximum boundary curvature is located somewhere along the curved boundary segment that connects the points where the circular patch intersects the boundary, but is not necessarily at the midpoint of this segment.

4.2. **Multiple Patches and the Effect of Fragmentation.** Next, for a fixed value of the constraint in (4.1), we consider the effect of both the location and the fragmentation of resources on the leading-order term, μ_0, in the asymptotic expansion of λ in (3.27) of Principal Result 3.1. The analysis below leads to three specific qualitative results. The following simple lemma is central to the derivation of these results:

Lemma 4.4: *Consider two smooth functions $C_{old}(\zeta)$ and $C_{new}(\zeta)$ defined on $0 \le \zeta < \mu_m^{old}$ and $0 \le \zeta < \mu_m^{new}$, respectively, with $C_{old}(0) = C_{new}(0) < 0$, and $C_{old}(\zeta) \to +\infty$ as $\zeta \to \mu_m^{old}$ from below, and $C_{new}(\zeta) \to +\infty$ as $\zeta \to \mu_m^{new}$ from below. Suppose further that there exist unique roots $\zeta = \mu_0^{old}$ and $\zeta = \mu_0^{new}$ to $C_{old}(\zeta) = 0$ and $C_{new}(\zeta) = 0$ on the intervals $0 < \zeta < \mu_m^{old}$ and $0 < \zeta < \mu_m^{new}$, respectively. Then,*

- *Case I: If $\mu_m^{new} \le \mu_m^{old}$ and $C_{new}(\zeta) > C_{old}(\zeta)$ on $0 < \zeta < \mu_m^{new}$, then $\mu_0^{new} < \mu_0^{old}$.*
- *Case II: If $\mu_m^{new} \ge \mu_m^{old}$ and $C_{new}(\zeta) < C_{old}(\zeta)$ on $0 < \zeta < \mu_m^{old}$, then $\mu_0^{new} > \mu_0^{old}$.*

The proof of this lemma is a routine exercise in calculus and is omitted. We now use this simple lemma to obtain our three main qualitative results.

First, we suppose that the center of the j^{th} patch of radius $\varepsilon\rho_j$ with associated angle $\pi\alpha_j$ is moved to an unoccupied location, with the new patch having radius $\varepsilon\rho_k$ and associated angle $\pi\alpha_k$. To satisfy (4.1), we require that $\alpha_j m_j \rho_j^2 = \alpha_k m_k \rho_k^2$. The change in $\mathcal{B}(\zeta)$, with $\mathcal{B}(\zeta)$ as defined in (3.28), induced by this action is

$$\begin{aligned}\mathcal{B}_{\text{new}}(\zeta) - \mathcal{B}_{\text{old}}(\zeta) &= \frac{\pi\alpha_k m_k \rho_k^2}{2 - \zeta m_k \rho_k^2} - \frac{\pi\alpha_j m_j \rho_j^2}{2 - \zeta m_j \rho_j^2} \\ &= \pi \left(\frac{\alpha_j}{\alpha_k}\right) \frac{m_j^2 \rho_j^4 \zeta}{\left(2 - \zeta m_j \rho_j^2\right)\left(2 - \zeta m_k \rho_k^2\right)} \left(\alpha_j - \alpha_k\right) .\end{aligned} \tag{4.12}$$

Recall from §3 that $\mathcal{B}_{\rm old}(\zeta)=0$ has a positive root $\zeta=\mu_0^{\rm old}$ on $0<\zeta<\mu_{\rm m}^{\rm old}\equiv 2/(m_J\rho_J^2)$, where $m_J\rho_J^2$ was defined in (3.30).

Assume that $\alpha_j>\alpha_k$. For instance, this occurs when the center of an interior patch, for which $\alpha_j=2$, is moved to a smooth point on the domain boundary, for which $\alpha_k=1$. First, suppose that the patches are favorable so that $m_j>0$ and $m_k>0$. When $\alpha_j>\alpha_k$, it follows from the constraint $\alpha_j m_j\rho_j^2=\alpha_k m_k\rho_k^2$ that $m_k\rho_k^2>m_j\rho_j^2$, and so the first vertical asymptote for $\mathcal{B}_{\rm new}(\zeta)$ cannot be larger than that of $\mathcal{B}_{\rm old}(\zeta)$. Consequently, we define $m_K\rho_K^2\equiv\max\{m_J\rho_J^2,m_k\rho_k^2\}$, and from §3 we conclude that there is a unique root $\zeta=\mu_0^{\rm new}$ to $\mathcal{B}_{\rm new}(\zeta)=0$ on $0<\zeta<\mu_{\rm m}^{\rm new}\equiv 2/(m_K\rho_K^2)$. Since $\mu_{\rm m}^{\rm new}\le\mu_{\rm m}^{\rm old}$, and (4.12) shows that $\mathcal{B}_{\rm new}(\zeta)>\mathcal{B}_{\rm old}(\zeta)$ for $0<\zeta<\mu_{\rm m}^{\rm new}$, then Case I of Lemma 4.4 proves that $\mu_0^{\rm new}<\mu_0^{\rm old}$. Alternatively, for the situation where habitats are unfavorable, so that $m_j<0$ and $m_k<0$, then the first vertical asymptotes of $\mathcal{B}_{\rm old}(\zeta)$ and $\mathcal{B}_{\rm new}(\zeta)$ must be the same, since these asymptotes are defined only in terms of the favorable patches. For this case, (4.12) again shows that $\mathcal{B}_{\rm new}(\zeta)>\mathcal{B}_{\rm old}(\zeta)$ for $0<\zeta<2/(m_J\rho_J^2)$. Case I of Lemma 4.4 then establishes that $\mu_0^{\rm new}<\mu_0^{\rm old}$. ■

Therefore, we conclude that moving the center of an interior patch to a point on the domain boundary will decrease the leading-order term μ_0 in the asymptotic expansion of the principal eigenvalue λ in (3.27) of Principal Result 3.1. Moreover, for a convex domain with piecewise smooth boundary, Qualitative Result I together with Principal Result 4.1 shows that μ_0 will be reduced the most by the movement of an interior patch to a non-smooth boundary point with the smallest corner contact angle. Since this patch was chosen arbitrarily, it is clear that μ_0 is minimized by the placement of all interior patches to the boundary of the domain. We interpret this result qualitatively as follows:

Qualitative Result I: *The movement of either a single favorable or unfavorable habitat to the boundary of the domain is advantageous for the persistence of the species.*

Next, we consider the effect of fragmentation on species persistence. More specifically, we consider the effect of splitting the i^{th} patch, of radius $\varepsilon\rho_i$ and growth rate m_i, into two distinct patches, one with radius $\varepsilon\rho_j$ and growth rate m_j, and the other with radius $\varepsilon\rho_k$ and growth rate m_k. The condition $m_i\rho_i^2=m_j\rho_j^2+m_k\rho_k^2$ is imposed to satisfy the constraint (4.1). We assume that $\alpha_i=\alpha_j=\alpha_k$, so that we are either splitting an interior patch into two interior patches, or a boundary patch into two boundary patches, with each boundary patch centered at either a smooth point of $\partial\Omega$ or at a corner point of $\partial\Omega$ with the same contact angle. This action leads to the following qualitative result:

Qualitative Result II: *The fragmentation of one favorable interior habitat into two separate favorable interior habitats is not advantageous for species persistence. Similarly, the fragmentation of a favorable boundary habitat into two favorable boundary habitats with each either centered at either a smooth point of $\partial\Omega$, or at a corner point of $\partial\Omega$ with the same contact angle, is not advantageous. Finally, the fragmentation of an unfavorable habitat into two separate unfavorable habitats increases the persistence threshold λ.*

We prove this result for $\alpha_i = \alpha_j = \alpha_k$ as follows. First, consider the case where we are fragmenting one favorable habitat into two smaller favorable habitats. Then, $m_i > 0$, $m_j > 0$, and $m_k > 0$. For the original patch distribution, it follows from §3 that $\mathcal{B}_{\rm old}(\zeta) = 0$ has a positive root $\zeta = \mu_0^{\rm old}$ on $0 < \zeta < \mu_{\rm m}^{\rm old} \equiv 2/(m_J\rho_J^2)$, where $m_J\rho_J^2$ was defined in (3.30). Since, clearly, the first vertical asymptote for $\mathcal{B}_{\rm new}(\zeta)$ cannot be smaller than that of $\mathcal{B}_{\rm old}(\zeta)$ under this fragmentation, it follows from §3 that $\mathcal{B}_{\rm new}(\zeta) = 0$ has a positive root $\zeta = \mu_0^{\rm new}$ on $0 < \zeta < \mu_{\rm m}^{\rm new}$ with $\mu_{\rm m}^{\rm new} \geq \mu_{\rm m}^{\rm old}$. From (3.28), we then calculate under the constraint $m_i\rho_i^2 = m_j\rho_j^2 + m_k\rho_k^2$ that the change in $\mathcal{B}(\zeta)$ induced by this fragmentation action is

$$\begin{aligned}\mathcal{B}_{\rm new}(\zeta) - \mathcal{B}_{\rm old}(\zeta) &= \frac{\pi\alpha_i m_j\rho_j^2}{(2-\zeta m_j\rho_j^2)} + \frac{\pi\alpha_i m_k\rho_k^2}{(2-\zeta m_k\rho_k^2)} - \frac{\pi\alpha_i m_i\rho_i^2}{(2-\zeta m_i\rho_i^2)} \\ &= \frac{-\pi\alpha_i\zeta\left(m_j\rho_j^2 m_k\rho_k^2\right)\left[\left(2-\zeta m_j\rho_j^2\right)+\left(2-\zeta m_k\rho_k^2\right)\right]}{\left(2-\zeta m_i\rho_i^2\right)\left(2-\zeta m_j\rho_j^2\right)\left(2-\zeta m_k\rho_k^2\right)}.\end{aligned} \tag{4.13}$$

Hence, from (4.13), we have that $\mathcal{B}_{\rm new}(\zeta) < \mathcal{B}_{\rm old}(\zeta)$ on $0 < \zeta < \mu_{\rm m}^{\rm old} \equiv 2/(m_J\rho_J^2)$. Since, in addition $\mu_{\rm m}^{\rm new} \geq \mu_{\rm m}^{\rm old}$, it follows from Case II of Lemma 4.4 that $\mu_0^{\rm new} > \mu_0^{\rm old}$. This proves the first two statements of Qualitative Result II.

To prove the final statement of this result, we suppose that we are fragmenting an unfavorable habitat into two smaller unfavorable habitats, so that $m_i < 0$, $m_j < 0$, and $m_k < 0$. For this situation, the first vertical asymptotes of $\mathcal{B}_{\rm old}(\zeta)$ and $\mathcal{B}_{\rm new}(\zeta)$ are the same, and (4.13) again shows that $\mathcal{B}_{\rm new}(\zeta) < \mathcal{B}_{\rm old}(\zeta)$ on $0 < \zeta < \mu_{\rm m}^{\rm old} \equiv 2/m_J\rho_J^2$. By Case II of Lemma 4.4, we conclude that $\mu_0^{\rm new} > \mu_0^{\rm old}$, which proves the last statement of Qualitative Result II. ■

The combination of Qualitative Results I and II show that, given some fixed amount of favorable resources to distribute, the optimal strategy is to clump them all together at a point on the boundary of the domain, and more specifically at the corner point of the boundary (if any are present) with the smallest contact angle less than π degrees. This strategy will ensure that the value of μ_0, and consequently the leading-order term for λ, is as small as possible, thereby maximizing the range of diffusivities D in (1.1) for the persistence of the species.

Our final qualitative result addresses whether it is advantageous to fragment a single interior favorable habitat into a smaller interior favorable habit together with a favorable boundary habitat. To study this situation, we introduce the constraint

$$m_i\rho_i^2 = m_j\rho_j^2 + \frac{\alpha_k}{2}m_k\rho_k^2\,, \tag{4.14}$$

with $\alpha_i = \alpha_j = 2$, and $\alpha_k < 2$. The subscript i represents the original interior habitat, whereas j and k represent the new smaller interior habitat and new boundary habitat, respectively. It is not clear apriori whether this action is advantageous, given that fragmentation of a favorable interior habitat into two favorable interior habitats increases the persistence threshold λ, but the relocation of a favorable interior habitat to the boundary decreases λ. A sufficient condition to treat this case, together with two additional related results, are summarized as follows:

Qualitative Result III: *The fragmentation of one favorable interior habitat into a new smaller interior favorable habitat together with a favorable boundary habitat, is advantageous for species persistence when the boundary habitat is sufficiently strong in the sense that*

$$m_k\rho_k^2 > \frac{4}{2-\alpha_k}m_j\rho_j^2 > 0\,. \tag{4.15}$$

Such a fragmentation of a favorable interior habitat is not advantageous when the new boundary habitat is too weak in the sense that

$$0 < m_k\rho_k^2 < m_j\rho_j^2\,. \tag{4.16}$$

Finally, the clumping of a favorable boundary habitat and an unfavorable interior habitat into one single interior habitat is not advantageous for species persistence when the resulting interior habitat is still unfavorable.

To prove this result, we first impose the constraint (4.14), and then calculate from (3.28) that

$$\begin{aligned}
\mathcal{B}_{\rm new}(\zeta) - \mathcal{B}_{\rm old}(\zeta) &= \frac{2\pi m_j\rho_j^2}{(2-\zeta m_j\rho_j^2)} + \frac{\pi\alpha_k m_k\rho_k^2}{(2-\zeta m_k\rho_k^2)} - \frac{2\pi m_i\rho_i^2}{(2-\zeta m_i\rho_i^2)}\,,\\
&= \frac{\pi\alpha_k\zeta\beta_k}{(2-\zeta\beta_i)(2-\zeta\beta_j)(2-\zeta\beta_k)}\left[\begin{array}{c}(2-\alpha_k)\beta_k - 4\beta_j\\ +\zeta\beta_j\left(\beta_j + \dfrac{\alpha_k}{2}\beta_k\right)\end{array}\right], \qquad (4.17a)\\
&= \frac{\pi\alpha_k\zeta\beta_k}{(2-\zeta\beta_i)(2-\zeta\beta_j)(2-\zeta\beta_k)}\left[\begin{array}{c}2(\beta_k-\beta_j) - \beta_j(2-\zeta\beta_j)\\ -\dfrac{\alpha_k\beta_k}{2}(2-\zeta\beta_j)\end{array}\right], \qquad (4.17b)
\end{aligned}$$

where we have defined $\beta_i \equiv m_i\rho_i^2$, $\beta_j \equiv m_j\rho_j^2$, and $\beta_k \equiv m_k\rho_k^2$. There are three parameter ranges of interest, corresponding to the three statements in Qualitative Result III.

We first suppose that $\beta_i > 0$ and $\beta_k > \frac{4}{2-\alpha_k}\beta_j > 0$. Then, from (4.14), it follows that $\beta_i > \beta_j$, and

$$\beta_i < \frac{(2-\alpha_k)}{4}\beta_k + \frac{\alpha_k}{2}\beta_k = \beta_k - \frac{1}{2}\left(1 - \frac{\alpha_k}{2}\right)\beta_k\,,$$

so that $\beta_i < \beta_k$ since $0 < \alpha_k < 2$. It then readily follows that the first vertical asymptote $\mu_{\rm m}^{\rm new}$ and $\mu_{\rm m}^{\rm old}$ for $\mathcal{B}_{\rm new}(\zeta)$ and $\mathcal{B}_{\rm old}(\zeta)$, respectively, must satisfy $\mu_{\rm m}^{\rm new} \le \mu_{\rm m}^{\rm old}$. Furthermore, it follows from (4.17a) that $\mathcal{B}_{\rm new}(\zeta) > \mathcal{B}_{\rm old}(\zeta)$ on $0 < \zeta < \mu_{\rm m}^{\rm new}$. Consequently, Case I of Lemma 4.4 ensures that $\mu_0^{\rm new} < \mu_0^{\rm old}$. This establishes the first statement of Qualitative Result III.

Secondly, we suppose that $\beta_i > 0$ and $\beta_j > \beta_k > 0$. Then, from (4.14), it follows that $\beta_i > \beta_j$, and $\beta_i > \beta_k + \alpha_k\beta_k/2 > \beta_k$ since $0 < \alpha_k < 2$. The condition that $\beta_i > \beta_j$ and $\beta_i > \beta_k$ ensures that the first vertical asymptotes of $\mathcal{B}_{\rm new}(\zeta)$ and $\mathcal{B}_{\rm old}(\zeta)$ must satisfy $\mu_{\rm m}^{\rm new} \ge \mu_{\rm m}^{\rm old}$. Furthermore, it follows from (4.17b) that $\mathcal{B}_{\rm new}(\zeta) < \mathcal{B}_{\rm old}(\zeta)$ on $0 < \zeta < \mu_{\rm m}^{\rm old}$. Consequently, Case II of Lemma 4.4 yields that $\mu_0^{\rm old} < \mu_0^{\rm new}$. This establishes the second statement of Qualitative Result III.

Finally, we suppose that $\beta_j < 0$, $\beta_k > 0$, and $\beta_i = \beta_j + \alpha_k\beta_k/2 < 0$. Then, since $\beta_i < 0$, it follows that the first vertical asymptote $\mu_{\rm m}^{\rm old}$ for $\mathcal{B}_{\rm old}(\zeta)$ cannot occur from the $i^{\rm th}$ patch. The condition $\beta_k > 0$ then ensures that $\mu_{\rm m}^{\rm new} \le \mu_{\rm m}^{\rm old}$, where $\mu_{\rm m}^{\rm new}$ is the vertical asymptote of $\mathcal{B}_{\rm new}(\zeta)$. Furthermore, it follows from (4.17a) that $\mathcal{B}_{\rm new}(\zeta) > \mathcal{B}_{\rm old}(\zeta)$ on $0 < \zeta < \mu_{\rm m}^{\rm new}$. Consequently, Case I of Lemma 4.4 establishes that $\mu_0^{\rm old} < \mu_0^{\rm new}$, which proves the final statement of Qualitative Result III. ■

As a remark, we now give an interpretation of the first statement of Qualitative Result III in terms of the areas of the patches for the special case where $m_j = m_k = 1$. Then, from (4.15) it follows that the fragmentation of a favorable interior habitat is advantageous when the area $\varepsilon^2 A_k \equiv \pi\varepsilon^2\rho_k^2/2$ of a new favorable habitat centered at a smooth point of the boundary is at least twice as large as the area $\varepsilon^2 A_j \equiv \pi\varepsilon^2\rho_j^2$ of the new smaller favorable interior habitat. If the new boundary habit is located at a $\pi/2$ corner of the domain, for which $\alpha_k = 1/2$, then a sufficient condition for this fragmentation to be advantageous is when the area ratio satisfies $A_k/A_j = \rho_k^2/(4\rho_j^2) > 2/3$.

We now give a specific example to illustrate Qualitative Results I–III.

Example I: (The Unit Disk): Let Ω be the unit disk for which the Neumann Green's function and its regular part are explicitly available (see (B.1) and (B.2) of Appendix B). We will compare the two-term asymptotic formula for λ in (3.27) of Principal Result 3.1 for three different arrangements of favorable resources inside Ω with $m_b = 2$ and $m_j = 1$ for $j = 1, \ldots, n$. For each of the three arrangements

below, we have fixed the common value $\int_\Omega m\,dx = -\pi$ for the constraint in (4.1). First, we consider clumping the favorable resources into one interior patch centered at the origin of radius ε. Then, we substitute $m_+ = 1$, $m_b = 2$, $|\Omega| = \pi$, and $R(0;0) = -3/(8\pi)$ from (B.1b) of Appendix B, into (2.26a) to get

$$\lambda \sim \nu + \nu^2/2\,, \qquad \text{(interior patch)}\,, \tag{4.18}$$

where $\nu = -1/\log\varepsilon$. Next, consider the optimal case where the favorable resources are all concentrated at a patch of radius $\sqrt{2}\varepsilon$ that is centered on the boundary of the unit disk. Since Ω is a disk, any such boundary point x_0 yields the minimum value of λ. For this case, we substitute $m_+ = 1$, $m_b = 2$, $|\Omega| = \pi$, $\alpha_0 = 1$, $\rho_0 = \sqrt{2}$, and $R_s(x_0;x_0) = 1/(8\pi)$ from (B.2) of Appendix B, into (2.46a), to obtain

$$\lambda \sim \frac{\nu}{2} - \frac{\nu^2}{2}\left(\frac{3}{8} - \log\sqrt{2}\right)\,, \qquad \text{(boundary patch)}\,. \tag{4.19}$$

Next, we suppose that n favorable patches of a common smaller radius $\varepsilon/\sqrt{n}$ have centers at the equally spaced points $x_j = re^{2\pi ij/n}$ on a ring of radius $r < 1$, where $i = \sqrt{-1}$. In this case, we set $m_b = 2$, $|\Omega| = \pi$, $m_j = 1$, $\rho_j = 1/\sqrt{n}$, and $\alpha_j = 2$ for $j = 1,\dots,n$, in (3.31) for μ_0 and (3.27) for λ. In this way, we get $\mu_0 = n$, and that (3.27) reduces to

$$\lambda \sim n\nu - n\nu^2\left(q_n(r) + \frac{1}{2}\log n + \frac{1}{4}\right)\,, \qquad q_n(r) \equiv \frac{2\pi}{n^2}p_n(r)\,, \tag{4.20a}$$

where $p_n(r) \equiv ne^t\mathcal{G}^{(N)}e$. Here $e = (1,\dots,1)^t$, and $\mathcal{G}^{(N)}$ is the $n\times n$ Neumann Green matrix with matrix elements $\left(\mathcal{G}^{(N)}\right)_{ij} = G(x_i;x_j)$ for $i \neq j$ and $\left(\mathcal{G}^{(N)}\right)_{jj} = R(x_j;x_j)$, where $G(x_i;x_j)$ and $R(x_j;x_j)$ are the Neumann Green's function of (2.19), given explicitly for the unit disk in (B.1). For n equally spaced patch centers on a ring of radius $r < 1$, $p_n(r)$ can be calculated explicitly, and is given in Proposition 4.3 of [15]. In this way, we obtain that $q_n(r)$ in (4.20a) is given explicitly by

$$q_n(r) = r^2 - \frac{3}{4} - \frac{1}{n}\log\left(nr^{n-1}\right) - \frac{1}{n}\log\left(1-r^{2n}\right)\,. \tag{4.20b}$$

In Fig. 5(a) we compare the three different two-term expansions for λ versus ε, given in (4.18), (4.19), and (4.20) with $n = 4$ and ring radius $r = 1/2$, representing the three different spatial arrangements of favorable resources. In agreement with our predictions in Qualitative Results I and II, the best choice is to concentrate resources on the boundary of the domain, while clumping resources at the center of the domain provides a better alternative than fragmenting the favorable resources into four separate patches on a ring.

Next, we illustrate Qualitative Result III. We consider fragmenting a single interior patch solution of radius ε centered at the origin into a boundary patch of radius

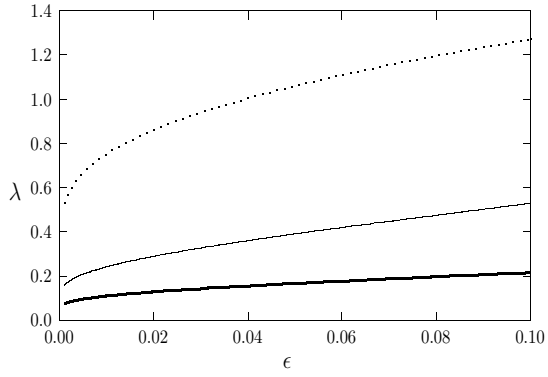

(a) λ versus ε

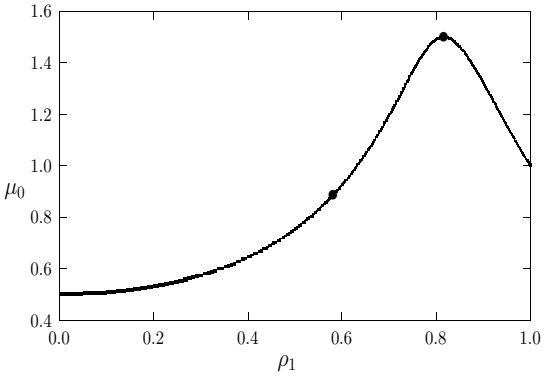

(b) μ_0 versus ρ_1

FIGURE 5. Example 1: Choose $m_b = 2$, and $m_j = 1$ for $j = 1, \ldots, n$, in the unit disk with $\int_\Omega m\,dx = -\pi$. Left figure: λ versus ε for three different cases: a single boundary patch (4.19) (heavy solid curve); a single interior patch centered at the origin (4.18) (solid curve); four small patches equally spaced on a ring of radius $r = 0.5$ (4.20) (dashed curve). The boundary patch gives the smallest λ, followed by the non-fragmented interior patch solution. Right figure: the leading order coefficient μ_0 versus ρ_1 from (4.21b) for the partial fragmentation of an interior patch of radius ε into a smaller interior patch of radius $\varepsilon\rho_1$ together with a boundary patch of radius $\varepsilon\rho_0$, while maintaining $\int_\Omega m\,dx = -\pi$. The bullets indicate the bounds from (4.15) and (4.16) of Qualitative Result III. Fragmentation is advantageous only when $\rho_1 < \sqrt{2/5}$.

$\varepsilon\rho_0$ and a smaller interior patch of radius $\varepsilon\rho_1$, while maintaining $\int_\Omega m\,dx = -\pi$. Thus, we require that ρ_0 and ρ_1, with $0 < \rho_1 < 1$, satisfy the constraint

$$1 = \rho_1^2 + \frac{1}{2}\rho_0^2\,. \tag{4.21a}$$

As remarked following (3.31), for a two-patch problem (3.28) reduces to a quadratic equation. We obtain that

$$\mu_0^2\rho_1^2\left(1-\rho_1^2\right)+\mu_0\left(-2+\frac{5}{2}\rho_1^2-\frac{3}{2}\rho_1^4\right)+1=0\,. \tag{4.21b}$$

Notice that $\mu_0=1$ when $\rho_1=1$, and $\mu_0=1/2$ when $\rho_1=0$, as expected. A plot of the smallest root to (4.21b) versus ρ_1 is shown in Fig. 5(b). The bound (4.16) in Qualitative Result III states that the partial fragmentation of the interior patch into a boundary patch is undesirable when $\rho_1>\rho_0$, which yields $\rho_1>\sqrt{2/3}$ from (4.21a). Alternatively, (4.15) together with (4.21a) shows that such a fragmentation is advantageous when $\rho_1<1/\sqrt{3}$. These two bounds are shown by the bullets in Fig. 5(b). For this simple two-patch case, we can readily show from the exact result (4.21b) that $\mu_0=1$ when $\rho_1=\sqrt{2/5}$, or equivalently $\rho_0=\sqrt{6/5}$. Thus, fragmentation is advantageous when $\rho_1<\sqrt{2/5}$, or equivalently $\rho_0>\sqrt{6/5}$.

Finally, we illustrate Qualitative Result III for the case where the unit disk has one pre-existing favorable interior patch of radius ε and growth rate $m_+=1$, together with one pre-existing unfavorable interior patch of radius ε and growth rate $m_-=-1$. We then introduce an additional favorable resource with local growth rate $m_0=1$ that can occupy an area ε^2A_0 if it is separated from the other two patches. We choose the bulk decay rate as $m_b=3$. We then compare three different options for using this additional favorable resource, subject to the constraint that $\int_\Omega m\,dx=-3\pi+A_0$ remains fixed. If we concentrate the additional favorable resource at a smooth point on the boundary, then from (3.28) μ_0 satisfies

$$-3+2\left(\frac{1}{2-\mu_0}-\frac{1}{2+\mu_0}\right)+\frac{A_0/\pi}{1-\mu_0A_0/\pi}=0\,. \tag{4.22a}$$

Alternatively, if the additional favorable resource is used to strengthen the pre-existing favorable interior patch, then from (3.28) μ_0 satisfies

$$-3+\frac{2\rho_+^2}{2-\rho_+^2\mu_0}-\frac{2}{2+\mu_0}=0\,,\qquad \rho_+^2=1+A_0/\pi\,. \tag{4.22b}$$

Finally, if the additional favorable resource is used to diminish the strength of the unfavorable pre-existing interior patch, then μ_0 satisfies

$$-3+\frac{2}{2-\mu_0}+\frac{m_-}{2-m_-\mu_0}=0\,,\qquad m_-=-1+A_0/\pi\,. \tag{4.22c}$$

In Fig. 6 we plot the three curves for μ_0 versus A_0/π as obtained from (4.22a)–(4.22c). A zoom of Fig. 6(a) for a subrange of A_0/π is shown in Fig. 6(b). We conclude that inserting a favorable boundary patch is preferable only when it has a sufficiently large size, and that if one only has a limited amount of an additional favorable resource it is preferable to re-enforce the pre-existing favorable habitat. In addition, Fig. 6(b) shows that it is not optimal for any range of A_0/π to use

the additional favorable resource to mitigate the effect of the unfavorable interior patch.

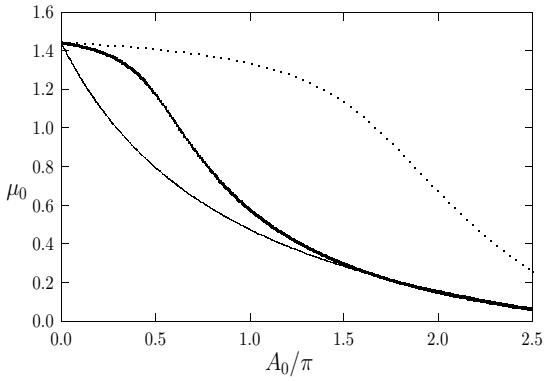

(a) μ_0 versus A_0/π

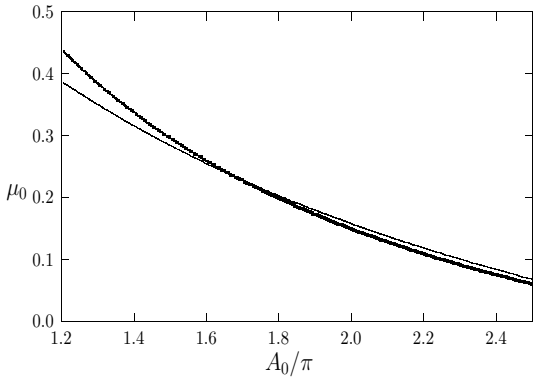

(b) μ_0 versus A_0/π

FIGURE 6. Example 1: Choose $m_b = 3$ and consider a pre-existing patch distribution of one favorable interior patch of local growth rate $m_+ = 1$ and radius ε and an unfavorable interior patch of local growth rate $m_- = -1$ and radius ε. Assume that we have an additional favorable resource of local growth rate $m_0 = 1$ that can occupy an area $\varepsilon^2 A_0$ if it separated from the two pre-existing interior patches. We plot μ_0 versus A_0/π when the additional resource is on the domain boundary (4.22a) (heavy solid curve), when it is used to re-enforce the existing favorable interior patch (4.22b) (solid curve), and when it is used to mitigate the effect of the unfavorable interior patch (4.22c) (dashed curve).

4.3. **Optimization at Second Order.** The minimization of λ in (3.27) is typically accomplished from the optimization of the coefficient μ_0 of the leading-order $\mathcal{O}(\nu)$

term in its asymptotic expansion. However, in certain degenerate cases, such as if a fixed distribution of interior patches is already present in the domain, the problem of optimizing the persistence threshold λ can require a careful examination of the coefficient μ_1 of the $\mathcal{O}(\nu^2)$ term in the asymptotic expansion of λ in (3.27). The coefficient μ_1 has an explicit dependence on the patch locations and accounts for interaction effects between the patches. An optimization problem of this type occurs in choosing the best location to place an additional favorable resource in a square domain. If this resource is sufficiently strong, then to minimize μ_0 it should be centered on the boundary of the square at a $\pi/2$ corner, and should not be used to strengthen a pre-existing favorable interior patch. In the situation where no other interior patches are present, each of the four corners of the square offers an equally good location to concentrate resources. However, if a distribution of fixed patches is already present in the domain, the best choice of corner to place an additional favorable patch is not clear apriori, and will depend on the spatial configuration of the fixed pre-existing patch distribution. In this case, the information required to make the optimal choice is provided by μ_1, which takes into account the interaction between the patches.

To formulate this restricted optimization problem, we let x_j for $j = 1, \ldots, n$ be the fixed pre-existing configuration of the centers of n circular patches in the interior of the domain with local growth rates m_j for $j = 1, \ldots, n$, where m_j is either positive (favorable habitat) or negative (unfavorable habit). We then introduce a new favorable habitat, and we assume that μ_0 is smallest when this additional habitat is located on the boundary of the domain. We then consider the problem of determining the optimal boundary location, x_0, of the center of one additional circular patch of radius $\varepsilon\rho_0$ and local growth rate $m_0 > 0$ and angle $\pi\alpha_0$. We showed earlier that to optimize μ_0, x_0 should be centered at a boundary point with the smallest contact angle $\pi\alpha_0$. In degenerate situations where this point is not uniquely determined, we must optimize the coefficient of the $\mathcal{O}(\nu^2)$ term in (3.27). To do so, we label $x_{n+1} = x_0$ and block the $(n+1)\times(n+1)$ matrices in (3.27) into an $n \times n$ block, labeled by $\mathcal{G}_m$ and $\mathcal{P}$, representing the fixed patch distribution, and a term $p(x_0)$ representing the interaction of the fixed patch distribution with the additional favorable resource. This determines μ_1 in (3.27) as

$$\mu_1 = \mu_0 \left(-\frac{1}{4} + \frac{\kappa^t \left(\mathcal{P} - \pi\mathcal{G}_m\right)\kappa + \kappa_0^2 \log\rho_0 - \pi p(x_0)}{\kappa^t\kappa + \kappa_0^2} \right) . \tag{4.23a}$$

In terms of the fixed distribution of patches, $\kappa = (\kappa_1, \ldots, \kappa_n)^t$, where κ_j for $j = 1, \ldots, n$ is defined in (3.22), while $\mathcal{G}_m$ and $\mathcal{P}$ are the $n \times n$ matrices as defined in (3.23). The scalar $p(x_0)$ in (4.23a), representing the interaction of the additional

favorable boundary patch, centered at x_0, with the fixed patch distribution is given by

$$p(x_0) = \alpha_0\kappa_0^2 R_m(x_0;x_0) + 2\sum_{j=1}^{n}\sqrt{\alpha_0\alpha_j}\kappa_0\kappa_j G_m(x_j;x_0)\,, \qquad \kappa_0 \equiv \frac{\sqrt{\alpha_0}m_0\rho_0^2}{2-\mu_0 m_0\rho_0^2}\,, \tag{4.23b}$$

where $\alpha_j = 2$ for $j = 1,\dots,n$. From (3.28), the leading-order coefficient μ_0 in the asymptotic expansion of λ is the smallest positive root of

$$-m_b|\Omega| + \pi\sqrt{\alpha_0}\kappa_0 + \pi\sum_{j=1}^{n}\sqrt{\alpha_j}\kappa_j = 0\,, \qquad \kappa_j \equiv \frac{\sqrt{\alpha_j}m_j\rho_j^2}{2-\mu_0 m_j\rho_j^2}\,, \quad j = 1,\dots,n\,. \tag{4.24}$$

The minimization of the persistence threshold λ corresponds to determining the location of the maximum of $p(x_0)$ for $x_0 \in \partial\Omega$. We now illustrate the problem of maximizing $p(x_0)$ for two specific examples.

Example 2: Pre-Existing Patch Distribution (Unit Disk): We first let Ω be the unit disc and $x_0 \in \partial\Omega$, for which $\alpha_0 = 1$. Since $x_0 \in \partial\Omega$, then $G_m(x_j;x_0) = G_s(x_j;x_0)$ and $R_m(x_0;x_0) = R_s(x_0;x_0)$ are the surface Neumann Green's function and its regular part given explicitly in (B.2). Now consider placing the centers x_j for $j = 1,\dots,n$ of the fixed patches on a ring of radius r so that $x_j = r\exp(2\pi ij/n)$ and $\alpha_j = 2$ for $j = 1,\dots,n$, with $0 < r < 1$. Then, from (4.23b) and (B.2), and with $\alpha_0 = 1$, we obtain

$$\begin{aligned} p(x_0) &= \frac{\kappa_0^2}{8\pi} + 2\kappa_0\sum_{j=1}^{n}\sqrt{\alpha_j}\kappa_j\left[\frac{r^2}{4\pi} - \frac{1}{8\pi} - \frac{1}{2\pi}\log|x_j - x_0|^2\right]\,, \\ &= \frac{\kappa_0^2}{8\pi} + \frac{\kappa_0}{2\pi}\left(r^2 - \frac{1}{2}\right)\sum_{j=1}^{n}\sqrt{\alpha_j}\kappa_j - \frac{\sqrt{2}\kappa_0}{\pi}\sum_{j=1}^{n}\kappa_j\log|x_j - x_0|^2\,, \\ &= \frac{\kappa_0^2}{8\pi} + \frac{\kappa_0}{2\pi}\left(r^2 - \frac{1}{2}\right)(m_b - \kappa_0) - \frac{\sqrt{2}\kappa_0}{\pi}\sum_{j=1}^{n}\kappa_j\log|x_j - x_0|^2\,, \end{aligned} \tag{4.25}$$

where in the last equality we have used the identity $\sum_{j=1}^{n}\sqrt{\alpha_j}\kappa_j = m_b - \kappa_0$ from (4.24). Finally, we write $x_0 = e^{i\theta_0}$ and calculate the logarithmic interaction term in (4.25) to get $p = p(\theta_0)$, where

$$p(\theta_0) = \frac{\kappa_0^2}{8\pi} + \frac{\kappa_0}{2\pi}\left(r^2 - \frac{1}{2}\right)(m_b - \kappa_0) - \frac{\sqrt{2}\kappa_0}{\pi}\sum_{j=1}^{n}\kappa_j\log\left(r^2 + 1 - 2r\cos\left(\theta_0 - \frac{2\pi j}{n}\right)\right)\,. \tag{4.26}$$

We now determine the location of the maximum value of $p(\theta_0)$ in (4.26), corresponding to the optimum location to insert the additional favorable resource on the boundary of the unit disk.

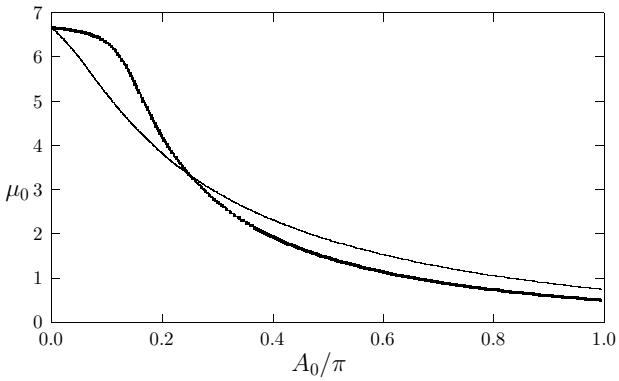

FIGURE 7. Example 2: Choose $m_b = 3$ and center five patches each of radius $\varepsilon/\sqrt{5}$ equidistantly on a ring of radius $r = 1/2$ in the unit disk with $m_j = 1$ for $j = 1, \ldots, 5$. Plot of μ_0, defined as the root of (3.28), versus A_0/π for an additional patch of area $\varepsilon^2 A_0$ located on the boundary of the domain (heavy solid curve) or used to re-enforce any one of the interior patches (solid curve). The boundary patch is preferable when $A_0/2 = 1/2$, which corresponds to the boundary patch radius $\rho_0 = 1$. The bound (4.15) states that the boundary patch is favorable when its radius satisfies $\rho_0 > 2/\sqrt{5}$ (or $A_0/\pi > 2/5$), while from (4.16) the boundary patch is not favorable when $\rho_0 < 1/\sqrt{5}$ (or $A_0/\pi < 1/10$).

We first suppose that $m_j = m_c$ for $j = 1, \ldots, n$, so that $\kappa_j = \kappa_c$ for $j = 1, \ldots, n$. Then, we write (4.26) as

$$p(\theta_0) = \frac{\kappa_0^2}{8\pi} + \frac{\kappa_0}{2\pi}\Big(r^2 - \frac{1}{2}\Big)(m_b - \kappa_0) - \frac{\sqrt{2}\kappa_0\kappa_c}{\pi}\chi(\theta_0)\,,$$
$$\chi(\theta_0) \equiv \sum_{j=1}^{n} \log\left[r^2 + 1 - 2r\cos\left(\theta_0 - \frac{2\pi j}{n}\right)\right]. \tag{4.27}$$

We then calculate that

$$\chi(\theta_0) = \sum_{j=1}^{n} \log\left[\left(r - \cos\left(\theta_0 - \frac{2\pi j}{n}\right)\right)^2 + \sin^2\left(\theta_0 - \frac{2\pi j}{n}\right)\right] = 2\log\Big(\prod_{j=1}^{n}|r - z_j|\Big)$$
$$= 2\log|r^n - e^{in\theta_0}| = \log\left[(r^n - \cos(n\theta_0))^2 + \sin^2(n\theta_0)\right], \tag{4.28}$$

where $z_j \equiv e^{i(\theta_0 - 2\pi j/n)}$. In obtaining the second to last equality in (4.28), we used the fact that z_j are the roots of $r^n - e^{in\theta_0} = 0$. Upon differentiating (4.28), it readily follows that the critical points of $\chi(\theta_0)$, and therefore $p(\theta_0)$, satisfy $\sin(n\theta_0) = 0$, which admits the $2n$ solutions

$$\theta_0 = \frac{2\pi j}{n}, \qquad \theta_0 = \frac{\pi(2j-1)}{n}, \qquad j = 1, \ldots, n\,, \tag{4.29}$$

on the interval $0 < \theta_0 \le 2\pi$. When $\kappa_c > 0$ in (4.27), then $\theta_0 = 2\pi j/n$ for $j = 1, \ldots, n$, clearly correspond to maxima of $p(\theta_0)$, while the remaining critical points in (4.29) are minima of $p(\theta_0)$. This result shows that when $\kappa_c > 0$, for which the ring is composed of n equally distributed favorable patches, the optimal boundary locations for the one additional favorable patch centered at x_0 is at the shortest distance to any of the n favorable habits on the ring. This result for $p(\theta_0)$ is illustrated by the heavy solid curve of Fig. 8(a) for $n = 5$ pre-existing patches for the parameter set $m_b = 3$, $m_0 = 1$, $\rho_0 = 1$, and with $m_j = 1$ and $\rho_j = 1/\sqrt{5}$ for $j = 1, \ldots, 5$. For this parameter set, where the favorable boundary patch is sufficiently strong in the sense of (4.15) of Qualitative Result III, μ_0 is indeed minimized when the favorable resource is concentrated on the boundary of the domain, rather than being used to re-enforce an interior favorable habitat. In Fig. 7 we plot μ_0 versus A_0/π, where $\varepsilon^2 A_0$ is the area of the additional favorable habitat for the case where the habitat is located on the boundary, and for the case when it is used to re-enforce one of the pre-existing favorable interior habitats. From this plot, we observe that a boundary habitat with $\rho_0 = 1$ and $A_0/\pi = 1/2$ provides $\mu_0 = 1.455$, which is the smaller of the two values for μ_0.

Alternatively, when $\kappa_c < 0$, only the locations $\theta_0 = \pi(2j-1)/n$ for $j = 1, \ldots, n$ correspond to maxima of $p(x_0)$. For this case, where the ring is composed of n equally spaced unfavorable habitats, the optimal boundary locations for the one additional favorable patch centered at x_0 is such that it maximizes the distance to any of the n unfavorable habitats on the ring. This result for $p(\theta_0)$ is illustrated by the solid curve in Fig. 8(a) for $n = 5$ pre-existing patches for the parameter set $m_b = 3$, $m_0 = 1$, $\rho_0 = 1$, and with $m_j = -1$ and $\rho_j = 1/\sqrt{5}$ for $j = 1, \ldots, 5$. For this parameter set $\mu_0 = 1.740$.

Finally, we consider n patches of a common radius $\varepsilon\rho_c$ but with $m_j = -m_c$ for $j = 1, \ldots, n-1$, and $m_n > 0$, where $m_c > 0$. Therefore, there are $n-1$ unfavorable habitats on the ring, with the only favorable habitat on the ring being centered at $x_n = (r, 0)$. For this case, $p(\theta_0)$ is given by (4.26) provided that we replace κ_j in (4.26) with

$$\kappa_j \equiv -\frac{\sqrt{2} m_c \rho_c^2}{2 + \mu_0 m_c \rho_c^2}\,, \quad j = 1, \ldots, n-1\,, \qquad \kappa_n \equiv \frac{m_n \rho_c^2}{2 - \mu_0 m_n \rho_c^2}\,. \tag{4.30}$$

A simple calculation from (4.26) shows that the maximum of $p(\theta_0)$ occurs at $\theta_0 = 0$. Therefore, the best location for the favorable boundary habitat is to insert it as close as possible to the only favorable interior habitat on the ring, which effectively decreases the effect of fragmentation. This result for $p(\theta_0)$ is illustrated by the dashed curve in Fig. 8(b) for $n = 5$ pre-existing patches for the parameter set

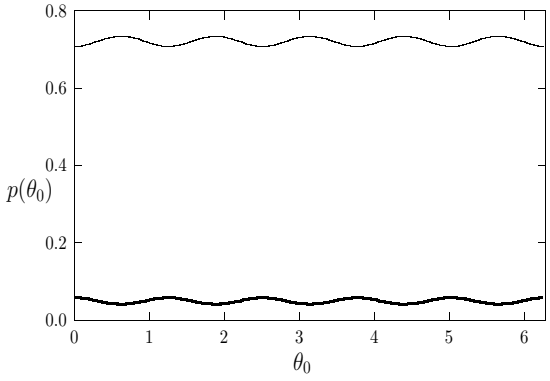

(a) $p(\theta_0)$ versus θ_0

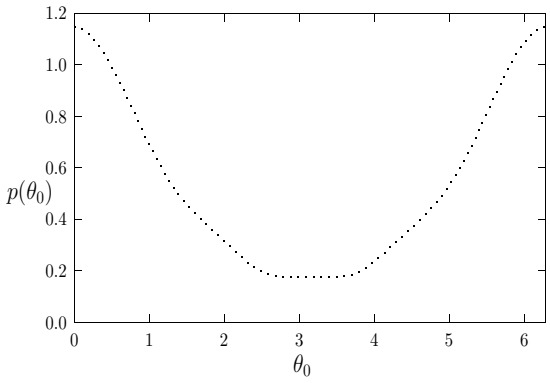

(b) $p(\theta_0)$ versus θ_0

FIGURE 8. Example 2: Choose $m_b = 3$ and center five patches each of radius $\varepsilon/\sqrt{5}$ equidistantly on a ring of radius $r = 1/2$ in the unit disk. Insert a favorable boundary patch of radius $\rho_0 = 1$ and growth rate $m_0 = 1$ at $x_0 = e^{i\theta_0}$ on the boundary of the unit disk. Left figure: $p(\theta_0)$ versus θ_0 from (4.26) for favorable interior patches (heavy solid curve) with $m_j = 1$ for $j = 1, \ldots, 5$, and for unfavorable interior patches (solid curve) with $m_j = -1$ for $j = 1, \ldots, 5$. Right figure: $p(\theta_0)$ versus θ_0 for four unfavorable interior patches with $m_j = -1$ for $j = 1, \ldots, 4$ and one favorable interior patch at $x_1 = (r, 0)$ with $m_5 = 1$.

$m_b = 3$, $m_0 = 1$, $\rho_0 = 1$, $m_j = -1$ and $\rho_j = 1/\sqrt{5}$ for $j = 1, \ldots, 4$, and $m_5 = 1$ with $\rho_5 = 1/\sqrt{5}$. For this parameter set $\mu_0 = 1.709$. From this figure we observe that $p(\theta_0)$ is minimized when $\theta_0 = \pi$, corresponding to the location on $\partial\Omega$ furthest from the only favorable interior habitat.

Example 3: Pre-Existing Patch Distribution (The Unit Square) For our final example we consider the problem of optimizing the location of one additional

favorable resource in the unit square domain $\Omega = [0,1] \times [0,1]$ given a certain distribution of pre-existing patches. This optimization problem is somewhat simpler than the previous example for the unit disk, since if the patch is sufficiently strong, the optimization of μ_0 requires that the additional resource be located at the corner x_0 of the square that maximizes $p(x_0)$ in (4.23b). For the unit square, explicit analytical formulae for the Neumann Green's function and its regular part required to optimize $p(x_0)$ in (4.23b) are given in Appendix B.

Let x_0 be the location of a patch of favorable resource with radius $\varepsilon\rho_0$ with $\rho_0 = 1$ and local growth rate $m_0 = 1$. We assume that there are four pre-existing patches in Ω centered at $x_1 = (1/4, 1/4)$, $x_2 = (1/4, 3/4)$, $x_3 = (3/4, 1/4)$, and $x_4 = (3/4, 3/4)$. Let each patch have a common radius $\varepsilon/2$ (i.e. $\rho_j = 1/2$ for $j = 1, \ldots, 4$) with local growth rate $m_1 = m_2 = m_3 = -1$, $m_4 = 1$, and the background decay rate $m_b = 3$. For this parameter set, where the favorable boundary patch is sufficiently strong in the sense of (4.15) of Qualitative Result III, μ_0 is minimized when the favorable resource is concentrated at one of the four corners on the square, rather than being used to re-enforce the only favorable interior habitat. By determining the root μ_0 of (3.28) numerically, we obtain that $\mu_0 = 1.605$ when the additional favorable resource is at a corner of the square, and $\mu_0 = 2.681$ when the additional favorable resource is used to strengthen the favorable resource at x_4. Therefore, μ_0 is smallest when x_0 is at a corner of the square. Then, by varying x_0 over the four corners of the square, we obtain the following numerical results for $p(x_0)$ from (4.23b):

$$x_0 = (0,0) \quad p(x_0) = -0.8522\,; \quad x_0 = (1,1) \quad p(x_0) = -0.2100\,.$$
$$x_0 = (1,0) \text{ or } x_0 = (0,1) \quad p(x_0) = -0.7163\,;$$

The largest value for $p(x_0)$ occurs when $x_0 = (1,1)$. Therefore, these results show that the persistence threshold λ is smallest when the additional favorable habitat is positioned at the corner of the square that is closest to the only favorable interior habitat. This action effectively decreases the effect of fragmentation.

5. **Discussion.** We have asymptotically calculated a two-term asymptotic expansion for the persistence threshold λ for the diffusive logistic model (1.1) in a highly patchy environment with spatially heterogeneous growth rate (1.4). The asymptotic result for λ is given in Principal Result 3.1 of §3. In the context of localized habitats, we have allowed for a relatively arbitrary spatial configuration of favorable and unfavorable habitats that are either interior to or on the boundary of a two-dimensional domain. We have examined in detail the effect of habitat fragmentation on the coefficient of the leading-order term in the asymptotic expansion of λ. Some general principles regarding the effect of fragmentation are summarized in

Qualitative Results I–III of §4. A few cases where the optimization of λ requires the examination of the higher-order coefficient in the asymptotic expansion of λ were also investigated.

There are two key problems that warrant further study. Firstly, it is highly desirable to provide a rigorous derivation of the asymptotic expansion for λ in Principal Result 3.1. Such a derivation could possibly be based on variational considerations and gamma convergence theory, similar to that used in [8] (see also the references therein) to analyze bubble solutions for the Cahn-Hillard equation of phase transition theory. Secondly, it would be interesting to extend our single-species analysis to the case of multi-species interaction, such as predator-prey interactions, for which a partial fragmentation of the prey habitat may become more beneficial for the persistence of the prey, rather than clumping the prey into a single habitat.

Acknowledgements. A. L. was supported by an NSERC graduate fellowship, and M. J. W. gratefully acknowledges the grant support of NSERC (Canada). M. J. W. would like to thank Profs. Chris Cosner, Steven Cantrell, and Mark Lewis, for suggesting the possible extension, mentioned in §5, of our one-species analysis to multi-species interactions. M. J. W. would also like to thank Prof. Anthony Peirce for providing the full numerical computations of the regular part of the Neumann Green's function given in Fig. 4 of §4.1. The proof of Principal Result 4.2 is due to Prof. Theodore Kolokolnikov, as originally reported in [20]. Finally, we would like to thank two anonymous referees for their detailed reading of the paper and their very helpful comments.

Appendix A. **The Regular Part of the Surface Neumann Green's Function for a Perturbed Disk.** In this appendix we give the proof of Principal Result 4.2 as obtained in [20]. In (2.42), we define $R_s(x;x_0)$ by $R_s(x;x_0) = G_s(x;x_0) + \pi^{-1}\log|x-x_0|$ for $x \in \partial\Omega$, where x_0 is at a smooth point of $\partial\Omega$. Then, we readily obtain from (2.42) that $R_s(x;x_0)$ satisfies

$$\Delta R_s(x;x_0) = \frac{1}{|\Omega|}\,, \qquad x\in\Omega\,; \qquad \nabla R_s(x;x_0)\cdot\hat{n} = \frac{1}{\pi}\frac{(x-x_0)\cdot\hat{n}}{|x-x_0|^2}\,, \qquad x\in\partial\Omega\,. \tag{A.1}$$

In polar coordinates we write $x_0 = (r_0\cos\theta_0, r_0\sin\theta_0)$, $x = (r\cos\theta, r\sin\theta)$, and $r_0 = r_0(\theta_0)$. We then calculate that $|x-x_0|^2 = r^2 + r_0^2 - 2rr_0\cos(\theta-\theta_0)$, and

$$\hat{n} = \frac{1}{\sqrt{(r')^2+r^2}}\begin{pmatrix} r'\sin\theta + r\cos\theta \\ -r'\cos\theta + r\sin\theta \end{pmatrix},$$

$$(x-x_0)\cdot\hat{n} = \frac{1}{\sqrt{(r')^2+r^2}}\left[r^2 - r_0r'\sin(\theta-\theta_0) - r_0r\cos(\theta-\theta_0)\right].$$

By writing $r = 1 + \delta\sigma$ and $r_0 = 1 + \delta\sigma_0$, the right-hand side of the boundary condition in (A.1) for $\delta \ll 1$ becomes

$$\frac{1}{\pi}\frac{(x-x_0)\cdot\hat{n}}{|x-x_0|^2} = \frac{1}{2\pi}\left(1+\delta\left[\frac{\sigma\cos(\theta-\theta_0)-\sigma_0-\sigma'\sin(\theta-\theta_0)}{1-\cos(\theta-\theta_0)}\right]\right)+\mathcal{O}(\delta^2)\,. \quad \text{(A.2)}$$

The expression in the square brackets above is bounded for $\theta \to \theta_0$. Therefore, (A.2) is uniformly valid for all $\theta \in [0, 2\pi)$. Next, we let $f(\theta)$ denote the term in the square brackets in (A.2) and we expand it in a Fourier series as

$$\begin{aligned} f(\theta) &\equiv \frac{\sigma\cos(\theta-\theta_0)-\sigma_0-\sigma'\sin(\theta-\theta_0)}{1-\cos(\theta-\theta_0)} \\ &= \sum_{m=1}^{\infty}\left[A_m\cos m(\theta-\theta_0)+B_m\sin m(\theta-\theta_0)\right]\,, \end{aligned} \quad \text{(A.3)}$$

where A_m and B_m for $m \geq 1$ are defined in terms of integrals I_1 and I_2, which must be calculated, by

$$I_1 \equiv \pi A_m = \int_0^{2\pi} f(\theta)\cos m(\theta-\theta_0)\,d\theta\,, \qquad I_2 \equiv \pi B_m \int_0^{2\pi} f(\theta)\sin m(\theta-\theta_0)\,d\theta\,. \quad \text{(A.4)}$$

Firstly, we consider the case where $\sigma = \cos n\theta = Re\left(e^{in\theta}\right)$. We write I_1 in (A.4) as

$$I_1 = Re\int_0^{2\pi}\left(\frac{\cos(\theta-\theta_0)e^{in\theta}-e^{in\theta_0}-ine^{in\theta}\sin(\theta-\theta_0)}{1-\cos(\theta-\theta_0)}\right)\cos m(\theta-\theta_0)\,d\theta\,.$$

Let $z = e^{i\theta}$, $z_0 = e^{i\theta_0}$, and $w = \frac{z}{z_0}$. Then, $I_1 = \mathrm{Re}(I)$, where I is the following contour integral over the unit disk:

$$I = iz_0^n\int_{|w|=1} G(w)\left(w^m + w^{-m}\right)\,dw\,,$$

$$G(w) \equiv \left(\frac{(1-n)}{2}w^{n+1}+\frac{(1+n)}{2}w^{n-1}-1\right)(1-w)^{-2}\,.$$

Since $(1-w)^2 = \frac{d}{dw}\sum_{n=0}^{\infty} w^n$, then

$$G(w) = -\left(1+2w+3w^2+\cdots+(n-1)w^{n-2}+\frac{(n-1)}{2}w^{n-1}+\cdots\right)\,.$$

From the residue theorem we calculate

$$I = z_0^n\begin{cases} 2\pi m\,, & 1\leq m<n \\ \pi(n-1)\,, & m=n \\ 0\,, & m>n \end{cases}\,, \quad \text{(A.5)}$$

so that $I_1 = \mathrm{Re}(I)$. Similarly, we can obtain I_2 when $\sigma = \cos(n\theta_0)$. In this way, we obtain

$$I_1 = \cos(n\theta_0)\begin{cases} 2\pi m\,, & 1\leq m<n \\ \pi(n-1)\,, & m=n \\ 0\,, & m>n \end{cases}\,, \quad I_2 = -\sin(n\theta_0)\begin{cases} 2\pi m\,, & 1\leq m<n \\ \pi(n-1)\,, & m=n \\ 0\,, & m>n \end{cases}\,.$$

Alternatively, for $\sigma = \sin(n\theta_0)$, we get

$$I_1 = \sin(n\theta_0)\begin{cases} 2\pi m\,, & 1 \le m < n \\ \pi(n-1)\,, & m = n \\ 0\,, & m > n \end{cases}, \quad I_2 = \cos(n\theta_0)\begin{cases} 2\pi m\,, & 1 \le m < n \\ \pi(n-1)\,, & m = n \\ 0\,, & m > n \end{cases}.$$

This determines A_n and B_n as $A_n = \frac{1}{\pi} I_1$ and $B_n = \frac{1}{\pi} I_2$. Therefore, for $\sigma = \cos(n\theta_0)$, (A.3) becomes

$$\begin{aligned} f(\theta) &= (n-1)\left(\cos n\theta_0 \cos n(\theta-\theta_0) - \sin n\theta_0 \sin n(\theta-\theta_0)\right) \\ &\quad + \sum_{m=1}^{n-1} 2m\left[\cos n\theta_0 \cos m(\theta-\theta_0) - \sin n\theta_0 \sin m(\theta-\theta_0)\right]. \end{aligned} \tag{A.6a}$$

Alternatively, for $\sigma = \sin(n\theta_0)$, (A.3) becomes

$$\begin{aligned} f(\theta) &= (n-1)\left(\cos n\theta_0 \sin n(\theta-\theta_0) + \sin n\theta_0 \cos n(\theta-\theta_0)\right) \\ &\quad + \sum_{m=1}^{n-1} 2m\left[\cos n\theta_0 \sin m(\theta-\theta_0) + \sin n\theta_0 \cos m(\theta-\theta_0)\right]. \end{aligned} \tag{A.6b}$$

Since $\sigma = \sum_{n=1}^{\infty}\left(a_n \cos n\theta + b_n \sin n\theta\right)$ from (4.3), we determine $f(\theta)$ by summing (A.6) over n. We then interchange the order of summation by using

$$\sum_{n=1}^{\infty}\sum_{m=1}^{n-1} \chi_{mn} = \sum_{n=1}^{\infty}\sum_{m>n}^{\infty} \chi_{nm}$$

to obtain

$$\begin{aligned} f(\theta) &= \sum_{n=1}^{\infty}\left(A_n \cos n(\theta-\theta_0) + B_n \sin n(\theta-\theta_0)\right), \\ A_n &= (n-1)\left(a_n \cos n\theta_0 + b_n \sin n\theta_0\right) + 2n\sum_{m>n}^{\infty}\left(a_m \cos m\theta_0 + b_m \sin m\theta_0\right), \\ B_n &= (n-1)\left(b_n \cos n\theta_0 - a_n \sin n\theta_0\right) + 2n\sum_{m>n}^{\infty}\left(b_m \cos m\theta_0 - a_m \sin m\theta_0\right). \end{aligned} \tag{A.7}$$

Next, we introduce $S(x;x_0)$ by

$$R_s(x;x_0) = S(x;x_0) + \frac{|x|^2}{4|\Omega|}. \tag{A.8}$$

By combining (A.8) and (A.1), we obtain that $S(x;x_0)$ satisfies

$$\begin{aligned} &\Delta S(x;x_0) = 0\,, \quad x \in \Omega\,; \\ &\partial_n S(x;x_0) = \partial_n\left[R_s(x;x_0) - \frac{|x|^2}{4|\Omega|}\right] \sim \frac{\delta}{2\pi}\left(f(\theta) - \sigma(\theta)\right) + \mathcal{O}(\delta^2)\,, \quad x \in \partial\Omega\,. \end{aligned} \tag{A.9}$$

In deriving the boundary condition in (A.9) we used (A.2), (A.3), $|\Omega| \approx \pi$, and $\partial_n\left(|x|^2\right) = 2r\left(1 + (r')^2/r^2\right)^{-1/2}$. The $\mathcal{O}(\delta)$ term in the boundary condition for S

in (A.9) suggests that we introduce $S_0(x;x_0)$ by

$$S(x;x_0) = \frac{\delta}{2\pi} S_0(x;x_0)\,. \tag{A.10}$$

To leading order we get $\partial_n S_0 = \partial_r S_0|_{r=1} + \mathcal{O}(\delta)$. From (A.9) and (A.10), we obtain that S_0 satisfies

$$\begin{aligned} &\Delta S_0(x;x_0) = 0\,, \qquad 0 \le r \le 1\,,\ 0 \le \theta < 2\pi; \\ &\partial_r S_0(x;x_0)|_{r=1} = f(\theta) - \sigma(\theta)\,, \qquad r = 1\,. \end{aligned} \tag{A.11}$$

The solution to (A.11) is written as

$$S_0 = D_0 + \sum_{n=1}^{\infty} r^n \left[D_n \cos n(\theta-\theta_0) + E_n \sin n(\theta-\theta_0) \right]\,. \tag{A.12}$$

To determine the coefficients D_n and E_n we must use the boundary condition in (A.11). To this end, we must re-write σ, given by equation (4.3), in terms of $\cos n(\theta-\theta_0)$ and $\sin n(\theta-\theta_0)$. This yields,

$$\begin{aligned} \sigma = &\sum_{n=1}^{\infty} \left[a_n \cos n\theta_0 + b_n \sin n\theta_0 \right] \cos n(\theta-\theta_0) \\ &+ \sum_{n=1}^{\infty} \left[b_n \cos n\theta_0 - a_n \sin n\theta_0 \right] \sin n(\theta-\theta_0)\,. \end{aligned} \tag{A.13}$$

Then, we differentiate (A.12) at $r = 1$, and use (A.7), (A.11), and (A.13), to determine D_n and E_n for $n \ge 1$ as

$$nD_n = A_n - \left[a_n \cos n\theta_0 + b_n \sin n\theta_0 \right]\,, \qquad nE_n = B_n - \left[b_n \cos n\theta_0 - a_n \sin n\theta_0 \right]\,. \tag{A.14}$$

We remark that the constant D_0 in (A.12) can be chosen to ensure that $\int_\Omega G(x;x_0)\,dx = 0$.

In summary, it follows from (A.8) and (A.10) that for $x \in \partial\Omega$,

$$R_s(x;x_0) = S(x;x_0) + \frac{|x|^2}{4\pi} = \frac{\delta}{2\pi} S_0(x;x_0) + \frac{1}{4\pi} + \frac{\delta\sigma}{2\pi} + \mathcal{O}(\delta^2)\,, \qquad x \in \partial\Omega\,.$$

By using the definition (4.4), and the reciprocity property of R_s, we calculate $\rho'(\theta_0)$ as

$$\begin{aligned} \rho'(\theta_0) &= \frac{d}{d\theta_0} R_s(x_0(\theta_0), x_0(\theta_0)) = 2\frac{d}{d\theta} R_s(x(\theta), x_0(\theta_0))|_{\theta=\theta_0} \\ &\sim \frac{\delta}{\pi} \left[\frac{d}{d\theta} S_0(x(\theta), x_0(\theta_0))|_{\theta=\theta_0} + \sigma'(\theta_0) \right] + \mathcal{O}(\delta^2)\,. \end{aligned}$$

Then, by using (A.12) and (A.13), we obtain

$$\rho'(\theta_0) = \frac{\delta}{\pi} \sum_{n=1}^{\infty} \left(nE_n + n\left[b_n \cos n\theta_0 - a_n \sin n\theta_0 \right] \right)\,.$$

Finally, we use (A.14) to relate E_n to B_n, and then recall (A.7) for B_n. This yields that

$$\rho'(\theta_0) = \frac{\delta}{\pi}\sum_{n=1}^{\infty}\left(2(n-1)\gamma_n + 2n\sum_{m>n}^{\infty}\gamma_m\right), \qquad \gamma_m = b_m\cos m\theta_0 - a_m\sin m\theta_0\,. \tag{A.15}$$

To simplify (A.15) we use the identity $\sum_{n=1}^{\infty}\sum_{m>n}^{\infty}2n\gamma_m = \sum_{m=2}^{\infty}\gamma_m\sum_{n=1}^{m-1}2n = \sum_{n=1}^{\infty}n(n-1)\gamma_n$. This yields the final result (4.6), and completes the proof of Principal Result 4.2. ■

Appendix B. **The Neumann and Surface Neumann Green's Function for a Disk and Square.** In this appendix we give analytical formulae for both the Neumann Green's function of (2.19) and the surface Neumann Green's function of (2.42) for the unit disk and the unit square.

Let $\Omega := \{x\,|\,|x|\le 1\}$ be the unit disk and represent the point $x\in\Omega$ as a complex number. Then, when $x_0\in\Omega$, we obtain from equation (4.3) of [15] that the Neumann Green's function of (2.19) and the self-interaction term R of (2.19b) are given explicitly by

$$G(x;x_0) = \frac{-1}{2\pi}\Big(\log|x-x_0| + \log\Big|x|x_0| - \frac{x_0}{|x_0|}\Big| - \frac{1}{2}(|x|^2+|x_0|^2) + \frac{3}{4}\Big), \tag{B.1a}$$

$$R(x_0;x_0) = \frac{-1}{2\pi}\left(\log\left(1-|x_0|^2\right) - |x_0|^2 + \frac{3}{4}\right). \tag{B.1b}$$

For $x_0\in\partial\Omega$, we obtain that the surface Green's function solution of (2.42) and its regular part in (2.42b) are given by

$$G_s(x;x_0) = -\frac{1}{\pi}\log|x-x_0| + \frac{|x|^2}{4\pi} - \frac{1}{8\pi}, \qquad R_s(x_0;x_0) = \frac{1}{8\pi}. \tag{B.2}$$

For the unit square Ω, we label $x=(x_1,x_2)$ as the observation point in $\Omega\equiv\{(x_1,x_2)\,|\,0<x_1<1\,,\,0<x_2<1\}$, while the singular point has coordinates $\xi = (\xi_1,\xi_2)$. Then, from Section §3.2 of [20], the Neumann Green's function with an interior singularity is given by

$$G(x;\xi) = -\frac{1}{2\pi}\log|x-\xi| + R(x;\xi)\,, \tag{B.3a}$$

where the regular part $R(x;\xi)$ is given explicitly by

$$\begin{aligned} R(x;\xi) = -\frac{1}{2\pi}\sum_{n=0}^{\infty}&\log(|1-q^n z_{+,+}||1-q^n z_{+,-}||1-q^n z_{-,+}||1-q^n\zeta_{+,+}| \\ &\times|1-q^n\zeta_{+,-}||1-q^n\zeta_{-,+}||1-q^n\zeta_{-,-}|) \\ &-\frac{1}{2\pi}\log\frac{|1-z_{-,-}|}{|r_{-,-}|} + H(x_1,\xi_1) - \frac{1}{2\pi}\sum_{n=1}^{\infty}\log|1-q^n z_{-,-}|\,. \end{aligned} \tag{B.3b}$$

Here the eight complex constants $z_{\pm,\pm}$ and $\zeta_{\pm,\pm}$ are defined in terms of additional complex constants $r_{\pm,\pm}$, $\rho_{\pm,\pm}$ by

$$z_{\pm,\pm} \equiv \mathrm{e}^{\pi r_{\pm,\pm}}\,, \quad \zeta_{\pm,\pm} \equiv \mathrm{e}^{\pi \rho_{\pm,\pm}}\,, \qquad q \equiv \mathrm{e}^{-2\pi} < 1\,, \tag{B.4a}$$

$$r_{+,\pm} \equiv -|x_1+\xi_1| + i(x_2 \pm \xi_2)\,, \qquad r_{-,\pm} \equiv -|x_1-\xi_1| + i(x_2 \pm \xi_2)\,, \tag{B.4b}$$

$$\rho_{+,\pm} \equiv |x_1+\xi_1| - 2 + i(x_2 \pm \xi_2)\,, \qquad \rho_{-,\pm} \equiv |x_1-\xi_1| - 2 + i(x_2 \pm \xi_2)\,. \tag{B.4c}$$

In (B.3) and (B.4), $|\omega|$ is the modulus of the complex number ω. In (B.3b), $H(x_1,\xi_1)$ is defined by

$$H(x_1,\xi_1) \equiv \frac{1}{12}\left[h(x_1-\xi_1) + h(x_1+\xi_1)\right]\,, \qquad h(\theta) \equiv 2 - 6|\theta| + 3\theta^2\,. \tag{B.5}$$

The self-interaction term $R(\xi;\xi)$, required in (2.19b) is obtained by setting $x=\xi$ in (B.3b).

Now suppose that the singular point is located on the bottom side of the square so that $\xi = (\xi_1, 0)$ with $0 < \xi_1 < 1$. Then, the term $\log|1-z_{-,+}|$ in (B.3b) also has a singularity at $x=(\xi_1,0)$, and must be extracted from the sum. In this case, the explicit solution to (2.19) is obtained by re-writing (B.3) as

$$G_s(x;\xi) = -\frac{1}{\pi}\log|x-\xi| + R_s(x;\xi)\,, \tag{B.6a}$$

where the regular part $R_s(x;\xi)$ is given explicitly by

$$\begin{aligned} R_s(x;\xi) = &-\frac{1}{2\pi}\sum_{n=0}^{\infty}\log(|1-q^n z_{+,+}||1-q^n z_{+,-}||1-q^n\zeta_{+,+}| \\ &\times |1-q^n\zeta_{+,-}||1-q^n\zeta_{-,+}||1-q^n\zeta_{-,-}|) \\ &-\frac{1}{2\pi}\log\frac{|1-z_{-,-}|}{|r_{-,-}|} - \frac{1}{2\pi}\log\frac{|1-z_{-,+}|}{|r_{-,+}|} + H(x_1,\xi_1) \\ &-\frac{1}{2\pi}\sum_{n=1}^{\infty}\log\left(|1-q^n z_{-,-}||1-q^n z_{-,+}|\right)\,. \end{aligned} \tag{B.6b}$$

The self-interaction term $R_s(\xi;\xi)$, required in (2.42b), is obtained by taking the limit $x \to \xi$ in (B.6b). By using L'Hopital's rule to calculate the terms $\log|1-z_{-,\pm}|/|r_{-,\pm}|$, we obtain with $q = e^{-2\pi}$ that

$$\begin{aligned} R_s(\xi;\xi) = &-\frac{1}{\pi}\sum_{n=0}^{\infty}\log\left[\left(1-q^n e^{-2\xi_1\pi}\right)\left(1-q^n e^{-2\pi(1-\xi_1)}\right)\right] \\ &-\frac{2}{\pi}\sum_{n=0}^{\infty}\log\left(1-q^n\right) - \frac{\log\pi}{\pi} + \left(\xi_1-\frac{1}{2}\right)^2 + \frac{1}{12}\,. \end{aligned} \tag{B.7}$$

A similar analysis can be done when ξ is on any of the other sides of the square.

Finally, suppose that $x_0 = (0,0)$ is at a corner of the square. Then, it is readily shown from (B.3) that $G_s(x;\xi)$ is

$$G_s(x;\xi) = -\frac{2}{\pi}\log|x| + R_s(x;0)\,, \tag{B.8a}$$

where the regular part $R_s(x;0)$ is given explicitly by

$$R_s(x;0) = -\frac{1}{2\pi}\sum_{n=1}^{\infty}\log\left(|1-q^n z_{+,+}||1-q^n z_{+,-}||1-q^n z_{-,+}||1-q^n z_{-,-}|\right)$$
$$-\frac{1}{2\pi}\sum_{n=0}^{\infty}\log\left(|1-q^n \zeta_{+,+}||1-q^n \zeta_{+,-}||1-q^n \zeta_{-,+}||1-q^n \zeta_{-,-}|\right)$$
$$-\frac{1}{2\pi}\log\left(\frac{|1-z_{+,+}|}{|r_{+,+}|}\frac{|1-z_{+,-}|}{|r_{+,-}|}\frac{|1-z_{-,+}|}{|r_{-,+}|}\frac{|1-z_{-,-}|}{|r_{-,-}|}\right)+H(x_1,0)\,. \quad \text{(B.8b)}$$

Moreover, the self-interaction term $R_s(0;0)$, required in (2.42b), is given by

$$R_s(0;0) = -\frac{4}{\pi}\sum_{n=1}^{\infty}\log\left(1-q^n\right)-\frac{2\log\pi}{\pi}+\frac{1}{3}\,, \qquad q=e^{-2\pi}\,. \quad \text{(B.9)}$$

REFERENCES

[1] H. Berestycki, F. Hamel, L. Roques, *Analysis of the Periodically Fragmented Environment Model: I - Species Persistence*, J. Math. Biol., **51**, No. 1, (2005), pp. 75–113.

[2] K. J. Brown, S. S. Lin, *On the Existence of Positive Eigenfunctions for an Eigenvalue Problem with Indefinite Weight Function*, J. Math. Anal. Appl., **75**, No. 1, (1980), pp. 112–120.

[3] A. Burchard, J. Denzler, *On the Geometry of Optimal Windows, with Special Focus on the Square*, SIAM J. Math. Anal., **37**, No. 6, (2006), pp. 1800-1827.

[4] R. S. Cantrell, C. Cosner, *Diffusive Logistic Equations with Indefinite Weights: Population Models in Disrupted Environments*, Proc. Roy. Soc. Edinburgh, **112A**, No. 3-4, (1989), pp. 293–318.

[5] R. S. Cantrell, C. Cosner, *Diffusive Logistic Equations with Indefinite Weights: Population Models in Disrupted Environments II*, SIAM J. Math. Anal., **22**, No. 4, (1991), pp. 1043–1064.

[6] R. S. Cantrell, C. Cosner, *The Effects of Spatial Heterogeneity in Population Dynamics*, J. Math. Biol., **29**, No. 4, (1991), pp. 315–338.

[7] R. S. Cantrell, C. Cosner, *Spatial Ecology via Reaction-Diffusion Systems*, Wiley Series in Mathematical and Computational Biology, John Wiley & Sons, Ltd., Chichester, 2003, xvi+411 pp.

[8] X. Chen, M. Kowalczyk, *Existence of Equilibria for the Cahn-Hilliard Equation via Local Minimizers of the Perimeter*, Comm. Partial Differential Equations, **21**, No. 7-8, (1996), pp. 1207-1233.

[9] D. Coombs, R. Straube, M. J. Ward, *Diffusion on a Sphere with Localized Traps: Mean First Passage Time, Eigenvalue Asymptotics, and Fekete Points*, SIAM J. Appl. Math., **70**, No. 1, (2009), pp. 302–332.

[10] A. M. Davis, S. G. Llewellyn Smith, *Perturbation of Eigenvalues due to Gaps in Two-Dimensional Boundaries*, Proc. Roy. Soc. A, **463**, No. 2079, (2007), pp. 759–786.

[11] J. Denzler, *Windows of Given Area with Minimal Heat Diffusion*, Trans. Amer. Math. Soc., **351**, No. 2, (1999), pp. 569-580.

[12] E. M. Harrell II, P. Kröger, K. Kurata, *On the Placement of an Obstacle or a Well so as to Optimize the Fundamental Eigenvalue*, SIAM J. Math. Anal., **33**, No. 1, (2001), pp. 240–259.

[13] P. Hess, *Periodic-Parabolic Boundary Value Problems and Positivity*, Pitman Research Notes in Mathematics, Vol. 247, Longman, Harlow, U.K. (1991).

[14] C. Y. Kao, Y. Lou, E. Yanagida, *Principal Eigenvalue for an Elliptic System with Indefinite Weight on Cylindrical Domains*, Math. Biosc. Eng. **5**, No. 2 (2008), pp. 315–335.

[15] T. Kolokolnikov, M. Titcombe, M. J. Ward, *Optimizing the Fundamental Neumann Eigenvalue for the Laplacian in a Domain with Small Traps*, European J. Appl. Math., **16**, No. 2, (2005), pp. 161–200.

[16] K. Kurata, J. Shi, *Optimal Spatial Harvesting Strategy and Symmetry-Breaking*, Appl. Math. Optim., **58**, No. 1, (2008), pp. 89–110.

[17] Y. Lou, E. Yanagida, *Minimization of the Principal Eigenvalue for an Elliptic Boundary Value Problem with Indefinite Weight and Applications to Population Dynamics*, Japan J. Indust. Appl. Math., **23**, No. 3, (2006), pp. 275–292.

[18] Y. Lou, *Some Challenging Mathematical Problems in Evolution of Dispersal and Population Dynamics*, Tutorials in Mathematical Biosciences. IV, 171–205, Lecture Notes in Math., **1922**, Springer, Berlin, (2008).

[19] S. Ozawa, *Singular Variation of Domains and Eigenvalues of the Laplacian*, Duke Math. J., **48**, No. 4, (1981), pp. 767-778.

[20] S. Pillay, M. J. Ward, A. Peirce, T. Kolokolnikov, *An Asymptotic Analysis of Mean First Passage Time Problems with Narrow Escape: Par I: Two-Dimensional Domains*, SIAM J. Multiscale Modeling, to appear, (2010), (28 pages).

[21] L. Roques, F. Hamel, *Mathematical Analysis of the Optimal Habitat Configurations for Species Persistence*, Math. Biosci., **210**, No. 1, (2007), pp. 34–59.

[22] L. Roques, R. Stoica, *Species Persistence Decreases with Habitat Fragmentation: An Analysis in Periodic Stochastic Environments*, J. Math. Biol., **2007**, No. 2, (2007), pp. 189–205.

[23] J. C. Saut, B. Scheurer, *Remarks on a Nonlinear Equation Arising in Population Genetics*, Comm. Part. Diff. Eq., **23**, (1978), pp. 907–931.

[24] N. Shigesada, K. Kawasaki, *Biological Invasions: Theory and Practice*, Oxford Series in Ecology and Evolution, Oxford: Oxford University Press, (1997).

[25] S. Senn, P. Hess, *On Positive Solutions of a Linear Elliptic Boundary Value Problem with Neumann Boundary Conditions*, Math. Ann. **258**, (1982), pp. 459–470.

[26] J. G. Skellam, *Random Dispersal in Theoretical Populations*, Biometrika, **38**, (1951), pp. 196–218.

[27] M. J. Ward, W. D. Henshaw, J. Keller, *Summing Logarithmic Expansions for Singularly Perturbed Eigenvalue Problems*, SIAM J. Appl. Math, Vol. 53, No. 3, (1993), pp. 799–828.

[28] M. J. Ward, J. B. Keller, *Strong Localized Perturbations of Eigenvalue Problems*, SIAM J. Appl. Math, Vol. 53, No. 3, (1993), pp. 770–798.

E-mail address: ael@math.ubc.ca

E-mail address: ward@math.ubc.ca